# Supporting Information

to

# Modulating the Guest Binding Ability within Mixed-Coordination Geometry $[Pd(\mu\text{-}L)_4RuCl_2]^{2+}$ and $[Pd(\mu\text{-}L)_4Pt]^{4+}$ Cage Architectures

Hayden B. Gearing,[a] Tilo Söhnel,[a,b] Paul Young,[c] Lynn Lisboa,[d] L. James Wright,[a] James D. Crowley,[b,d] and Christian G. Hartinger[a,*]

[a] School of Chemical Sciences, University of Auckland, Private Bag 92019, Auckland 1142 (New Zealand)

[b] MacDiarmid Institute for Advanced Materials and Nanotechnology, Victoria University of Wellington, PO Box 600, Wellington 6140 (New Zealand)

[c] School of Biological Sciences, University of Auckland, Private Bag 92019, Auckland 1142 (New Zealand)

[d] Department of Chemistry, University of Otago, PO Box 56, Dunedin 9054 (New Zealand)

## Table of Contents

## Experimental procedures

### General

Unless otherwise stated, all reagents were purchased from commercial sources and used without further purification. $[Pd(DMAP)_4](BF_4)_2$ and $[Pt(3\text{-}PA)_4](BF_4)_2$,[1,2] *N*-boc-3-aminobenzoic acid,[3] *trans*-$[Ru(DMSO)_4Cl_2]$,[4] and compound **1** were synthesised following a literature procedures.[2] Solvent and reagent abbreviations include acetonitrile (MeCN), dichloromethane (DCM), dimethylformamide (DMF), dimethylsulfoxide (DMSO), methanol (MeOH), ethyl acetate (EtOAc), diethyl ether ($Et_2O$), and 3-pyridinecarboxaldehyde (3-PA). $^1H$, $^{13}C\{^1H\}$, DEPTQ, COSY, NOESY, HSQC and DOSY (Table S1) NMR spectra were recorded in DMSO-$d_6$ or MeCN-$d_3$ on Bruker AVIII 400, 400plus or Ascend 500 NMR spectrometers at ambient temperatures. Chemical shifts (δ) are reported in parts per million (ppm). $^1H$ NMR spectra were referenced to residual solvent peaks; DMSO-$d_6$, δ 2.50 ppm; MeCN-$d_3$, δ 1.94 ppm. $^{13}C\{^1H\}$ NMR spectra were referenced to signals associated with DMSO-$d_6$ (δ 39.52 ppm). Note that the $^{13}C\{^1H\}$ DEPTQ spectra recorded in DMSO-$d_6$ with the Ascend 500 NMR spectrometer revealed the presence of DMSO-$d_4$ (pentet, δ 39.77 ppm). $^1H$ NMR spectroscopic data are reported as chemical shift, multiplicity (s, singlet; brs, broad singlet; d, doublet; dd, doublet of doublets; ddd, doublet of doublets of doublets; dt, doublet of triplets; t, triplet; td, triplet of doublets; hept, heptet; m, multiplet), coupling constant (*J*) in Hertz (Hz), relative integral, and assignment. Signals in the $^1H$ and $^{13}C\{^1H\}$ NMR spectra were assigned using a combination of 2D NMR experiments. HMBC spectra of compounds **1a**–**3b** were not of sufficient quality to assign quaternary carbons.

Electrospray ionisation mass spectrometry (ESI-MS) data were recorded on a Thermo Orbitrap Exploris 120 mass spectrometer in positive ionisation mode. For MSAs **1a**–**3b**, samples were run under cold-spray conditions with the desolvation temperature set to the lowest possible setting (50 °C).

Molecular structures were either determined by X-ray diffraction measurements (XRD) or micro electron diffraction (microED). XRD of single crystals of **2a**, **3a**, and **2b** were performed on a Rigaku Oxford Diffraction XtaLAB-Synergy-S single-crystal diffractometer (Rigaku Corp., Tokyo, Japan) with a PILATUS 200 K hybrid pixel array detector using Cu Kα radiation (λ = 1.54184 Å). The data were processed with the SHELXT[5] and Olex2[6,7] software packages (Tables

S3 and S4). All non-hydrogen atoms were refined anisotropically. Hydrogen atoms were inserted at calculated positions and refined with a riding model or without restrictions. Mercury 2022.1.0 was used to visualise the molecular structures.[8]

For microED data collection, microcrystalline samples of **a** and **3b** were ground in crystallisation solvent to produce small fragments suitable for ED analysis. A suspension of the microcrystalline samples (2 µL) was applied to a C-Flat Holey Carbon grid (1.2 µm hole, 1.3 µm space 300 mesh) over a vacuum to remove the solvent, and the grid plunged into liquid $N_2$. The TEM grid was loaded into a Gatan 626 high tilt cryo-holder and inserted into a Techni G2 F20 electron microscope operating at 200 kV (0.02508 Å wavelength). Samples were examined in low-dose search mode (1700x magnification) to isolate and centre microcrystals at eucentric height. For microED data collection, the microscope was set for electron diffraction (C2 lens intensity of 60% with an objective aperture size of 20 and selected area aperture of 200 µm) with a detector distance of 730 mm, which equates to a virtual detector distance of 975 mm. Continuous-rotation microED data were recorded in tiff format on a TVIPS 16k CMOS camera using a rolling shutter mode to collect 200 continuous exposures while the grid was rotated through 120 degrees (-60° to 60°). A TVIPS detector control module (MicroED.exe) was used to control the speed of the cryo-holder rotation so that each of the exposure frames (1.6 s) equated to 0.6° of crystal rotation. The datasets were converted from tiff to SMV format using guiEM2EM[9] and visually inspected with Adxv.[10] The data were indexed and integrated in XDS and multiple crystal datasets scaled and merged with XSCALE.[11] Reflection files were converted to SHELX hkl format with XDSCONV[11] and the ab initio structures were determined by SHELXT,[5] followed by refinement in SHELXL.[12] Hydrogen atoms were located at the geometrically idealised positions.

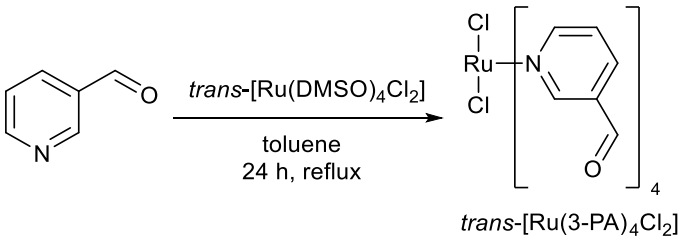


**Scheme S1.** Preparation of *trans*-[Ru(3-PA)$_4$Cl$_2$] **a**.

## Synthesis of tert-butyl(3-(nicotinamido)phenyl)carbamate

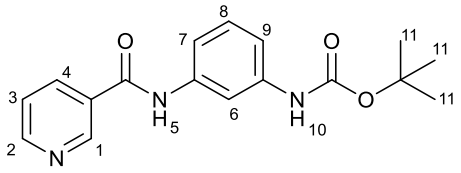

*N*-Boc-*m*-phenylenediamine (750 mg, 3.60 mmol), HATU (1.51 g, 3.96 mmol) and nicotinic acid (488 mg, 3.96 mmol) were suspended in acetonitrile (40 mL). Triethylamine (1.0 mL, 7.2 mmol) was added, and the reaction mixture stirred for 16 h at 60 °C under $N_2$ atmosphere. After cooling the reaction mixture to room temperature, the solvent was removed under reduced pressure and water (ca. 80 mL) was added. The crude reaction mixture was sonicated for 3–4 h. The resulting suspension was filtered, washed with water (4 × 25 mL) and dried by suction and *in vacuo* to yield the compound as a grey/brown powder (900 mg, 80%). $^{1}$H NMR (400 MHz, DMSO-$d_6$, 298 K) δ 10.41 (s, 1H, H-5), 9.39 (s, 1H, H-10), 9.09 (dd, *J* = 2.3, 0.7 Hz, 1H, H-1), 8.75 (dd, *J* = 4.8, 1.6 Hz, 1H, H-2), 8.35 – 8.22 (m, 1H, H-4), 8.01 (t, *J* = 1.9 Hz, 1H, H-6), 7.55 (ddd, *J* = 8.0, 4.8, 0.8 Hz, 1H, H-3), 7.47 – 7.36 (m, 1H, H-7), 7.21 (t, *J* = 8.1 Hz, 1H, H-8), 7.11 (ddd, *J* = 8.1, 1.8, 0.9 Hz, 1H, H-9), 1.48 (s, 9H, H-11). $^{13}$C{$^{1}$H} NMR (101 MHz, DMSO-$d_6$, 298 K) δ 164.0, 152.7, 152.0, 148.7, 139.8, 139.1, 135.4, 130.6, 128.6, 123.4, 114.4, 114.1, 110.5, 79.0, 28.1 ppm. ESI-MS: *m/z* 314.1498 ($[M + H]^+$ $m/z_{calc}$ 314.1499), 336.1314 ($[M + Na]^+$ $m/z_{calc}$ 336.1318), 627.2919 ($[2M + H]^+$ $m/z_{calc}$ 627.2924), 649.2735 ($[2M + H]^+$ $m/z_{calc}$ 649.2744).

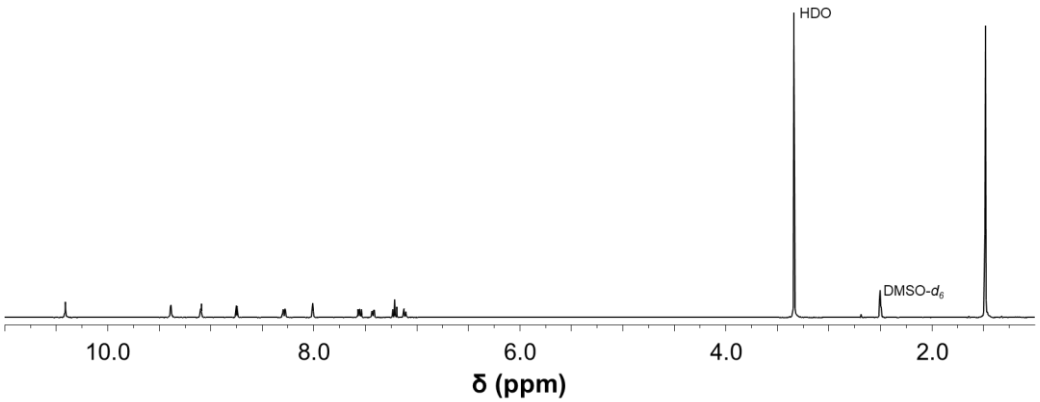


**Figure S1.** $^{1}$H NMR spectrum (400 MHz, DMSO-$d_6$, 298 K) of tert-butyl(3-(nicotinamido)phenyl)carbamate.

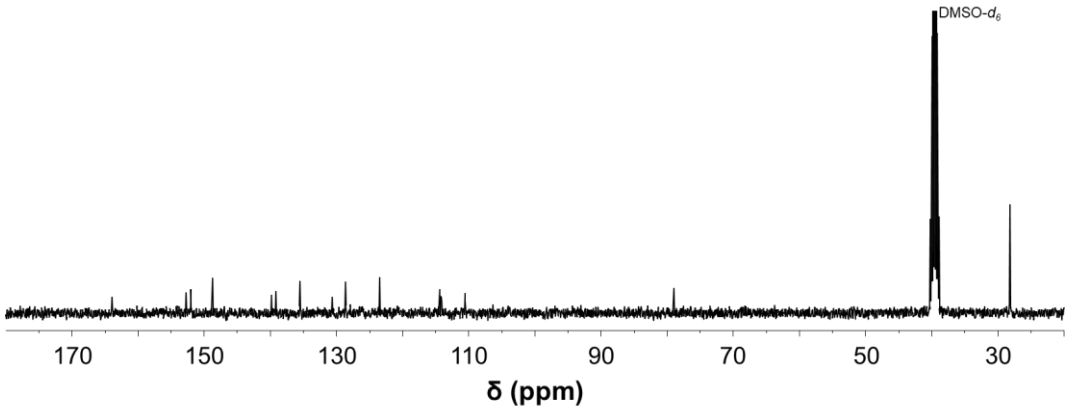


**Figure S2.** $^{13}$C{$^{1}$H} NMR spectrum (101 MHz, DMSO-$d_6$, 298 K) of tert-butyl(3-(nicotinamido)phenyl)carbamate.

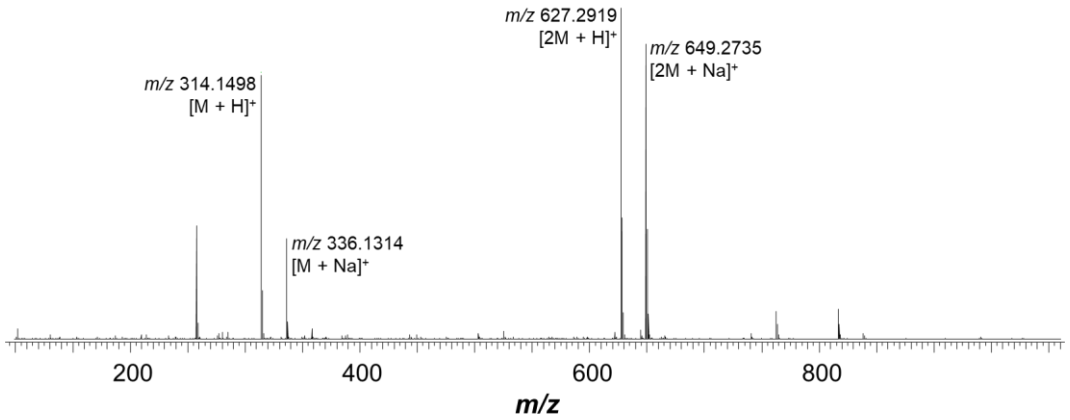


**Figure S3.** ESI-mass spectrum (MeOH) of tert-butyl(3-(nicotinamido)phenyl)carbamate.

## Synthesis of *N*-(3-aminophenyl)nicotinamide, **2**

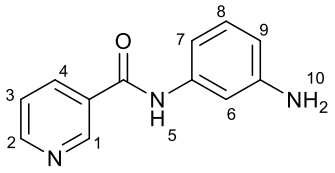


Tert-butyl(3-(nicotinamido)phenyl)carbamate (600 mg, 1.91 mmol) was added to chloroform (10 mL) followed by 2 mL of trifluoroacetic acid. The reaction mixture was stirred for 3 h and then solvent and trifluoroacetic acid were removed *in vacuo*. Saturated sodium bicarbonate solution (25 mL) was added to the residue and stirred until the evolution of $CO_2$ stopped. The aqueous solution was then extracted with dichloromethane (2 × 100 mL) and the organic layers were collected and combined, dried with $MgSO_4$, and filtered. The solvent was removed from the filtrate to yield **2** as an off-white powder (364 mg, 89%).$^{1}$H NMR (400 MHz, DMSO-$d_6$, 298 K) δ 10.13 (s, 1H, H-5), 9.06 (d, *J* = 1.7 Hz, 1H, H-1), 8.74 (dd, *J* = 4.8, 1.6 Hz, 1H, H-2), 8.33 – 8.16 (m, 1H, H-4), 7.54 (ddd, *J* = 7.9, 4.8, 0.6 Hz, 1H, H-3), 7.08 (t, *J* = 1.9 Hz, 1H, H-6), 6.97 (t, *J* = 7.9 Hz, 1H, H-8), 6.86 (d, *J* = 8.0 Hz, 1H, H-7), 6.41 – 6.26 (m, 1H, H-9), 5.11 (brs, 2H, H10). $^{13}$C{$^{1}$H} NMR (101 MHz, DMSO-$d_6$, 298 K) δ 163.8, 151.9, 149.0, 148.6, 139.4, 135.4, 130.9, 128.9, 123.4, 110.1, 108.3, 106.1 ppm. ESI-MS: *m/z* 214.0972 ([M + H]$^{+}$ $m/z_{calc}$ 214.0974), 236.0792 ([M + Na]$^{+}$ $m/z_{calc}$ 236.0794).

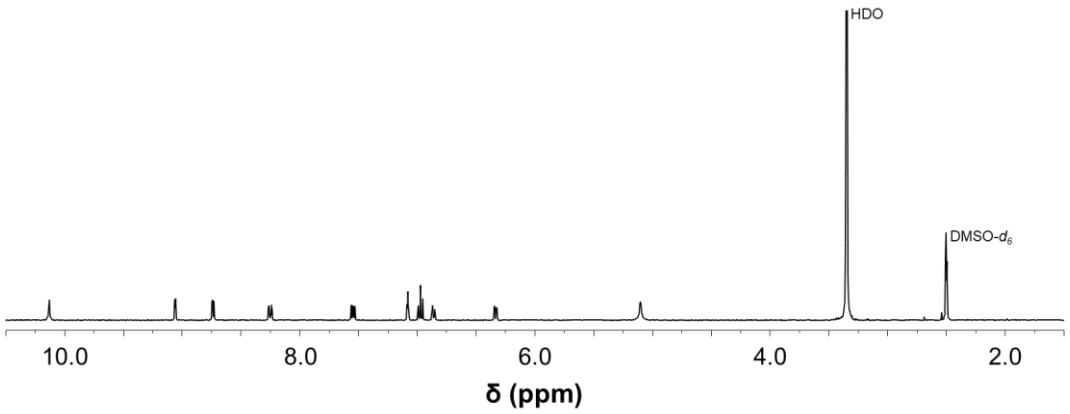


**Figure S4.** $^{1}$H NMR spectrum (400 MHz, DMSO-$d_6$, 298 K) of *N*-(3-aminophenyl)nicotinamide **2**.

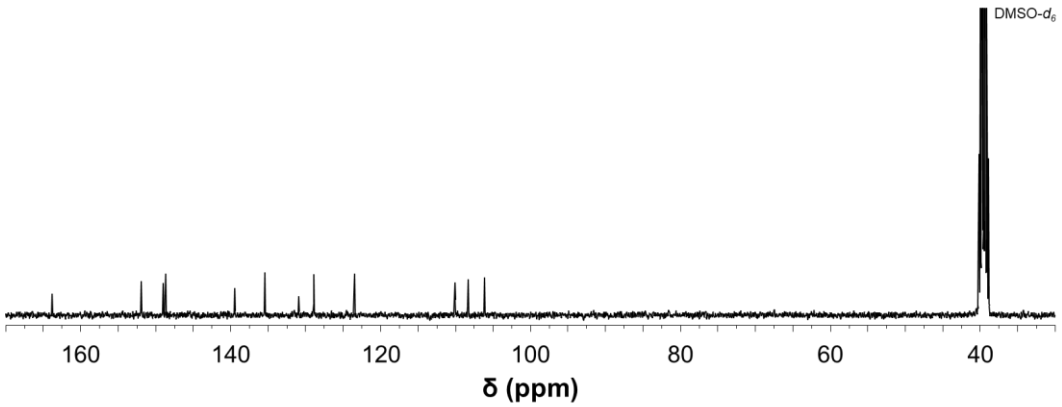


**Figure S5.** $^{13}C\{^{1}H\}$ NMR spectrum (101 MHz, DMSO-$d_6$, 298 K) of *N*-(3-aminophenyl)nicotinamide **2**.

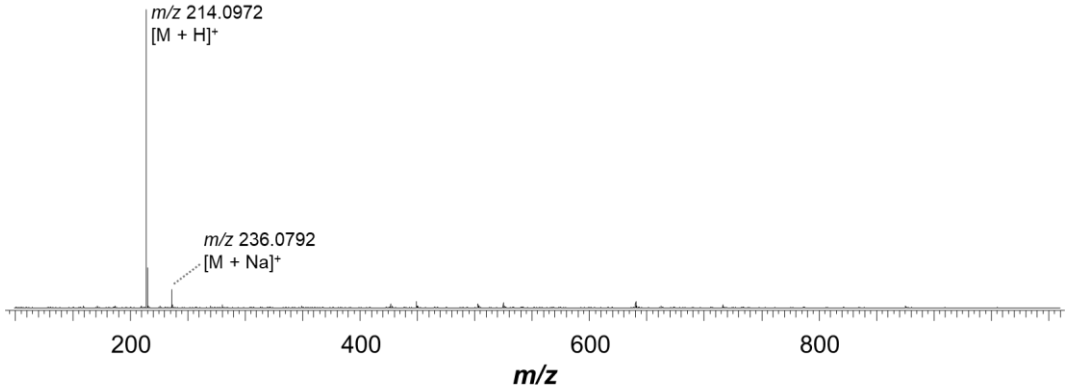


**Figure S6.** ESI-mass spectrum (MeOH) of *N*-(3-aminophenyl)nicotinamide **2**.

## Synthesis of tert-butyl(3-(pyridin-3-ylcarbamoyl)phenyl)carbamate

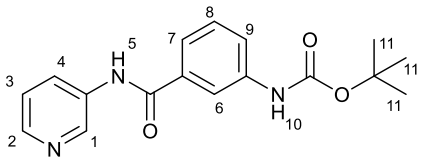

N-Boc-3-aminobenzoic acid (600 mg, 2.52 mmol) and HATU (960 mg, 2.56 mmol) were suspended in acetonitrile (60 mL), and triethylamine (0.388 mL, 2.78 mmol) was added. The resulting solution was stirred for approximately 20 min to activate the acid before 3-aminopyridine (238 mg, 2.52 mmol) was added. The reaction mixture was stirred under $N_2$ for 16 h at 60 °C, after which the acetonitrile was removed under reduced pressure. Water (50 mL) was added, and the crude product was sonicated for 3 h resulting in an off-white precipitate. The suspension was filtered, washed with water (4 × 25 mL) and dried *in vacuo* to

yield the product as an off-white solid (506 mg, 65 %). $^{1}$H NMR (400 MHz, DMSO-$d_6$, 298 K) δ 10.26 (s, 1H, H-5), 8.91 (dd, J = 2.4, 0.4 Hz, 1H, H-1), 8.28 (dd, J = 4.7, 1.5 Hz, 1H, H-2), 8.17 (ddd, J = 8.3, 2.6, 1.5 Hz, 1H, H-4), 7.37 (ddd, J = 8.4, 4.7, 0.7 Hz, 1H, H-3), 7.16 (t, J = 7.7 Hz, 1H, H-8), 7.12 – 7.04 (m, 2H, H-6 & H-7), 6.77 (ddd, J = 7.9, 2.3, 1.0 Hz, 1H, H-9) ppm. $^{13}$C NMR (101 MHz, DMSO-$d_6$, 298 K) δ 166.1, 152.8, 144.5, 142.0, 139.8, 135.8, 135.2, 128.7, 127.3, 123.5, 121.4, 121.1, 117.6, 79.3, 28.1. ESI-MS: *m/z* 314.1497 ([M + H]$^+$ $m/z_{calc}$ 314.1499), 627.2919 ([2M + H]$^+$ $m/z_{calc}$ 627.2924).

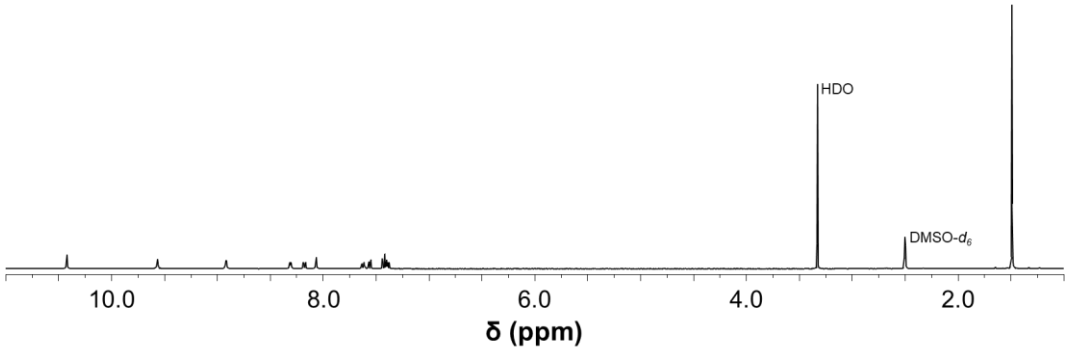


**Figure S7.** $^{1}$H NMR spectrum (400 MHz, DMSO-$d_6$, 298 K) of tert-butyl(3-(pyridin-3-ylcarbamoyl)phenyl)carbamate.

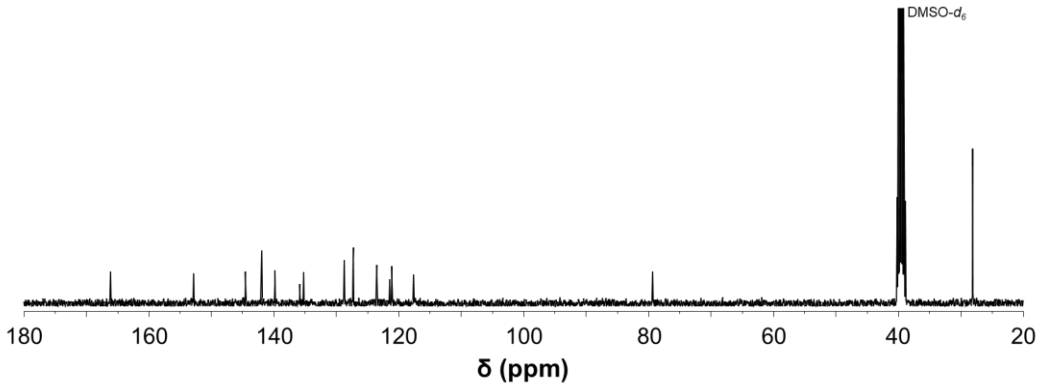


**Figure S8.** $^{13}$C{$^{1}$H} NMR spectrum (101 MHz, DMSO-$d_6$, 298 K) of tert-butyl(3-(pyridin-3-ylcarbamoyl)phenyl)carbamate.

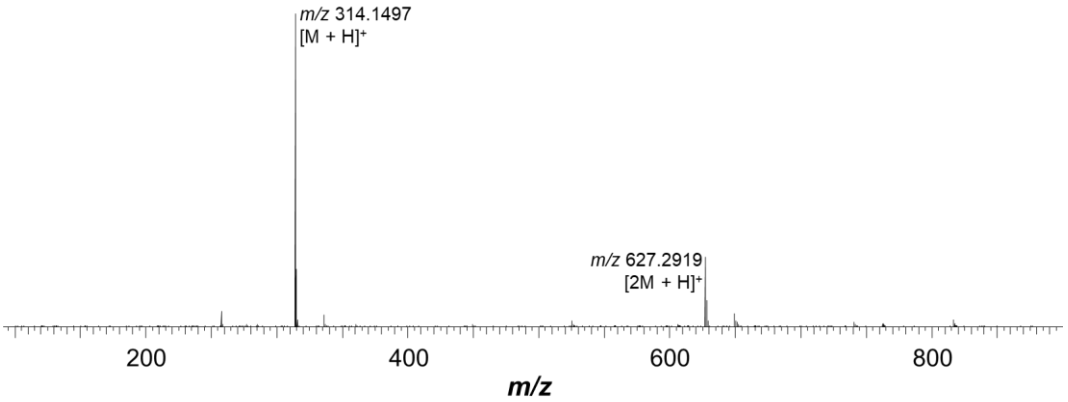


**Figure S9.** ESI-mass spectrum (MeOH) of tert-butyl(3-(pyridin-3-ylcarbamoyl)phenyl)carbamate.

## Synthesis of 3-amino-*N*-(pyridin-3-yl)benzamide **3**

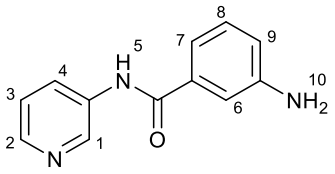


3-Amino-N-(pyridin-3-yl)benzamide was synthesised analogously to compound **2** using tert-butyl(3-(pyridin-3-ylcarbamoyl)phenyl)carbamate (600 mg, 1.91 mmol). Yield: 294 mg (72%), off-white powder. $^{1}$H NMR (400 MHz, DMSO-$d_6$, 298 K) δ 10.13 (s, 1H, H-5), 9.06 (dd, *J* = 2.3, 0.8 Hz, 1H, H-1), 8.73 (dd, *J* = 4.8, 1.7 Hz, 1H, H-2), 8.25 (ddd, *J* = 7.9, 2.2, 1.8 Hz, 1H, H-4), 7.54 (ddd, *J* = 7.9, 4.8, 0.8 Hz, 1H, H-3), 7.08 (t, *J* = 2.0 Hz, 1H), 6.97 (t, *J* = 7.9 Hz, 1H), 6.89 – 6.83 (m, 1H), 6.33 (ddd, *J* = 7.9, 2.2, 1.0 Hz, 1H), 5.10 (s, 2H). $^{13}$C NMR (101 MHz, DMSO-$d_6$, 298 K) δ 163.8, 151.9, 149.0, 148.6, 139.4, 135.4, 130.94 128.9, 123.4, 110.1, 108.3, 106.1 ppm. ESI-MS: *m/z* 214.0973 ([M + H]$^+$ $m/z_{calc}$ 214.0974).

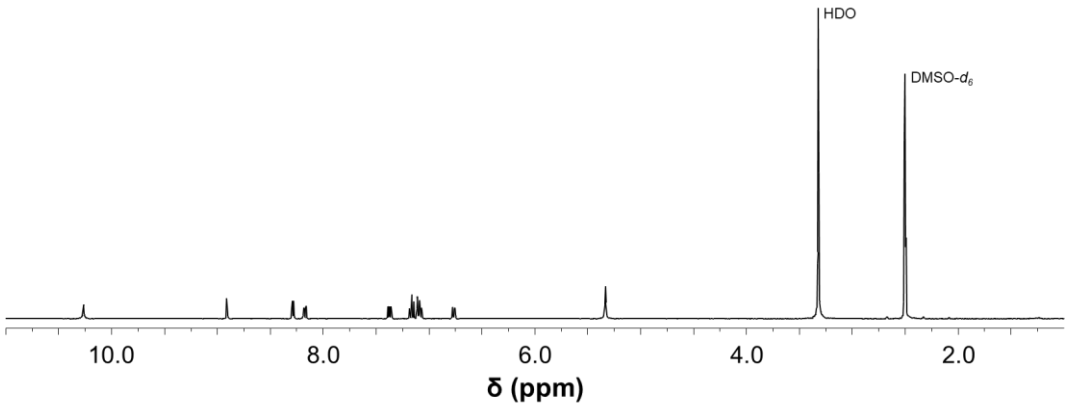


**Figure S10.** $^{1}$H NMR spectrum (400 MHz, DMSO-$d_6$, 298 K) of 3-amino-*N*-(pyridin-3-yl)benzamide **3**.

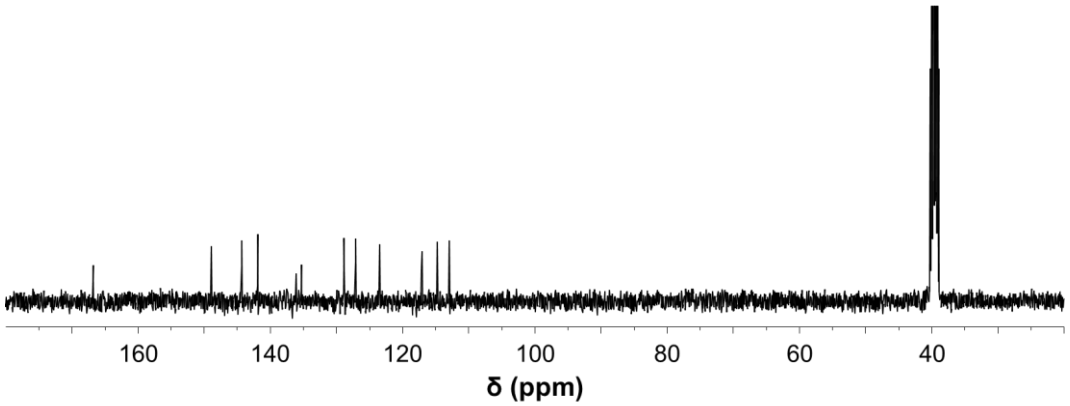


**Figure S11.** $^{13}$C{$^{1}$H} NMR spectrum (101 MHz, DMSO-$d_6$, 298 K) of 3-amino-*N*-(pyridin-3-yl)benzamide **3**.

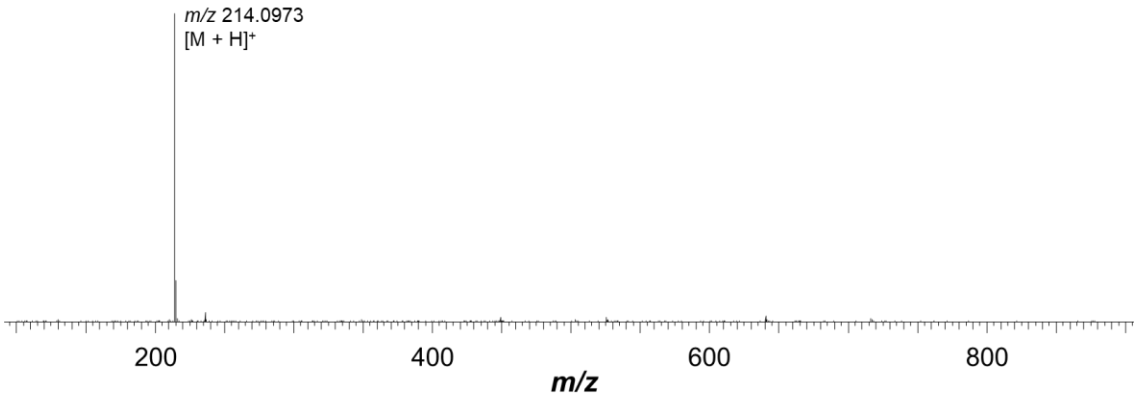


**Figure S12.** ESI-mass spectrum (MeOH) of 3-amino-*N*-(pyridin-3-yl)benzamide **3**.

Synthesis of *trans*-[dichloridotetrakis(3-pyridinecarboxaldehyde)ruthenium(II)] $[Ru(3\text{-}PA)_4Cl_2]$ **a**

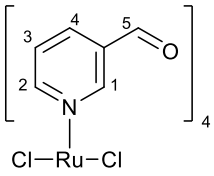


3-Pyridinecarboxaldehyde (1.44 mL, 15.4 mmol) was added to a suspension of *trans*-$[Ru(DMSO)_4Cl_2]$ (992 mg, 2.05 mmol) in toluene (50 mL) and the mixture was refluxed for 24 h. The solution was cooled to room temperature and the red precipitate filtered, washed with toluene until the washings were clear, then washed with $Et_2O$ (20 mL) and dried by suction to give **a** as a bright red powder (1.12 g, 91%). $^1$H NMR (400 MHz, DMSO-$d_6$, 298 K) δ 9.93 (s, 4H, H-5), 8.89 (d, *J* = 1.8 Hz, 4H, H-1), 8.66 (dd, *J* = 5.8, 1.0 Hz, 4H, H-2), 8.31 (dt, *J* = 7.8, 1.6 Hz, 4H, H-4), 7.53 (dd, *J* = 7.7, 5.8 Hz, 4H, H-3). $^{13}$C NMR (101 MHz, DMSO-$d_6$, 298 K) δ 191.6, 161.7, 157.9, 135.7, 131.6, 124.4 ppm. ESI-MS: *m/z* 599.9918 ($[M - 2BF_4]^{2+}$ $m/z_{calc}$ 599.9900).

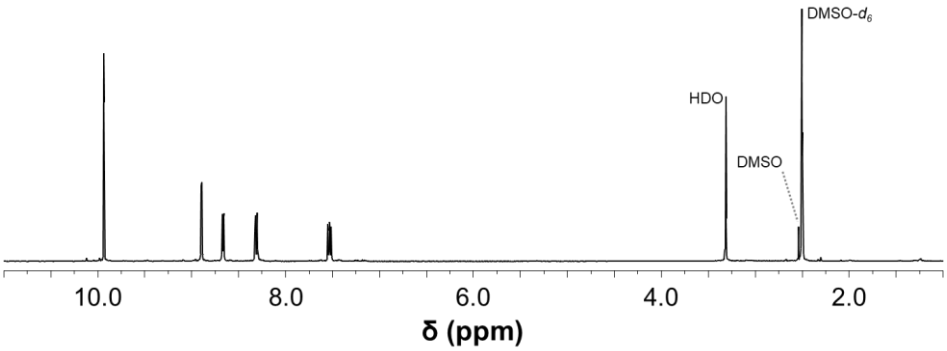


**Figure S13.** $^1$H NMR spectrum (400 MHz, DMSO-$d_6$, 298 K) of *trans*-[dichloridotetrakis(3-pyridinecarboxaldehyde)ruthenium(II)] **a**.

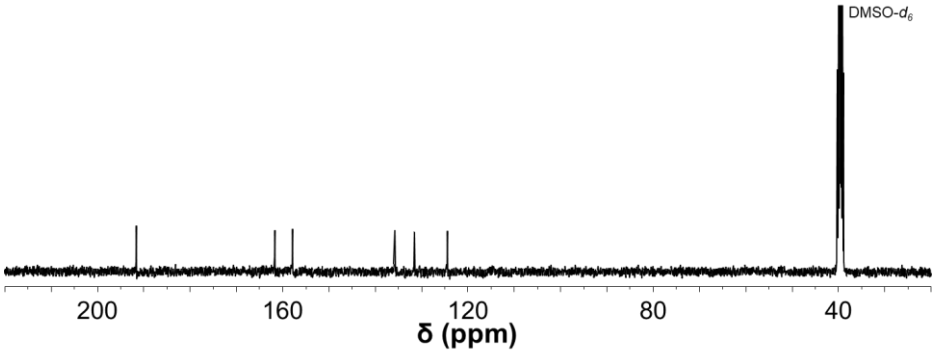


**Figure S14.** $^{13}C\{^{1}H\}$ NMR spectrum (101 MHz, DMSO-$d_6$, 298 K) of *trans*-[dichloridotetrakis(3-pyridinecarboxaldehyde)ruthenium(II)] **a**.

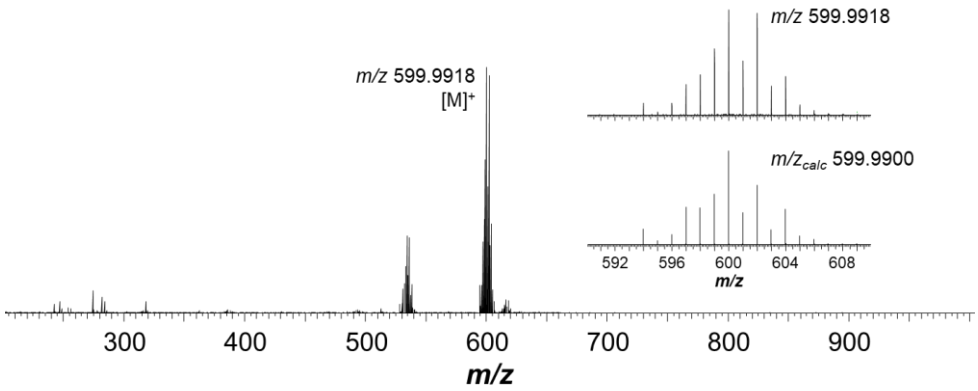


**Figure S15.** ESI-mass spectrum (DMSO/MeCN) of *trans*-[dichloridotetrakis(3-pyridinecarboxaldehyde)ruthenium(II)] **a**.

Synthesis of **1a**

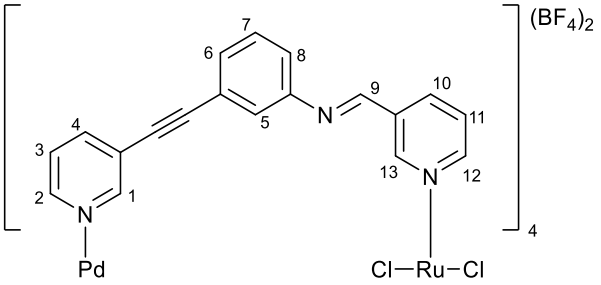


Compound **1** (75 mg, 0.386 mmol), $[Pd(MeCN)_4](BF_4)_2$ (43 mg, 0.097 mmol), and $[Ru(3\text{-}PA)_4Cl_2]$ **a** (58 mg, 0.097 mmol) were added to DMSO (4 mL), heated until all solids dissolved and stirred for 3 h protected from light. After addition of EtOAc (ca. 40 mL), the precipitate was filtered, washed with EtOAC (20 mL), and $Et_2O$ (20 mL) to yield **1a** as a red solid (109 mg, 71%). $^1$H NMR (400 MHz, DMSO-$d_6$, 298K) δ 9.52 (d, *J* = 1.4 Hz, 4H, H-1), 9.48 (d, *J* = 1.8 Hz, 4H, H-13), 9.37 (dd, *J* = 5.8, 1.0 Hz, 4H, H-2), 8.93 (dd, *J* = 5.9, 1.0 Hz, 4H, H-12), 8.56 (s, 4H, H-9), 8.24 – 8.15 (m, 8H, H-4 & H-10), 7.77 (dd, *J* = 8.0, 5.8 Hz, 4H, H-3), 7.53 – 7.36 (m, 20H, H-5, H-6, H-7, H-8 & H-11) ppm. $^{13}$C-DEPTQ NMR (126 MHz, DMSO-$d_6$, 298 K) δ 159.6 (C-9), 159.1 (C-12), 157.5 (C-13), 153.0 (C-1), 150.9 (Cq), 150.2 (C-2), 142.5 (C-10), 135.2 (C-4), 131.0 (Cq), 130.3 (C-5, 6, 7, 8, 11), 129.0 (C-5, 6, 7, 8, 11), 126.6 (C-3), 123.8 (C-5, 6, 7, 8, 11), 122.4 (Cq), 121.7 (Cq), 121.3 (C-5, 6, 7, 8, 11), 94.5 (Cq), 84.5 (Cq) ppm. ESI-MS: *m/z* 744.1064 ($[M - 2BF_4]^{2+}$ $m/z_{calc}$ 744.1060). ESI-MS: *m/z* 706.0947 ($[M - 2BF_4]^{2+}$ $m/z_{calc}$ 706.0943).

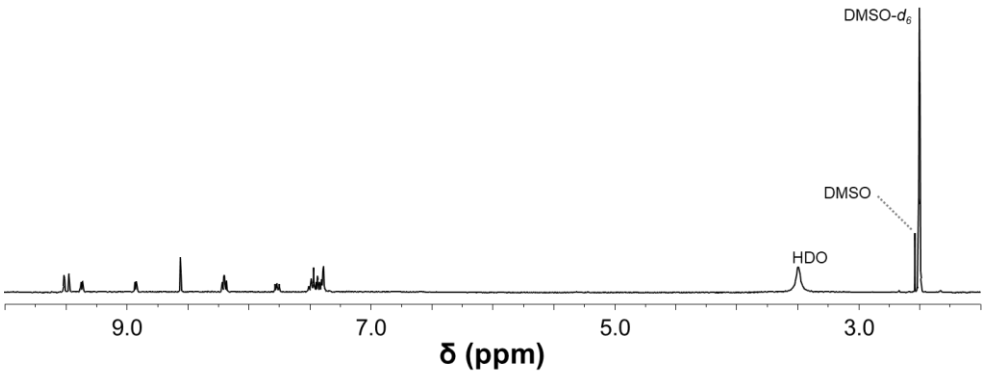


**Figure S16.** $^1$H NMR spectrum (400 MHz, DMSO-$d_6$, 298 K) of cage complex **1a**.

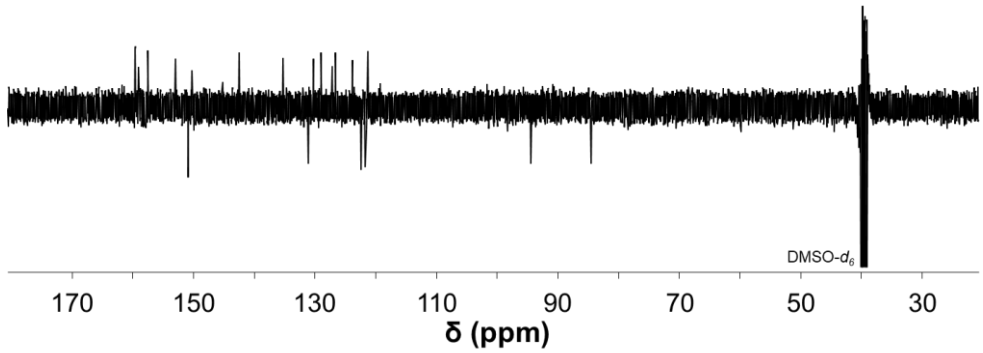


**Figure S17.** $^{13}C\{^{1}H\}$-DEPTQ NMR spectrum (126 MHz, DMSO-$d_6$, 298 K) of **1a**.

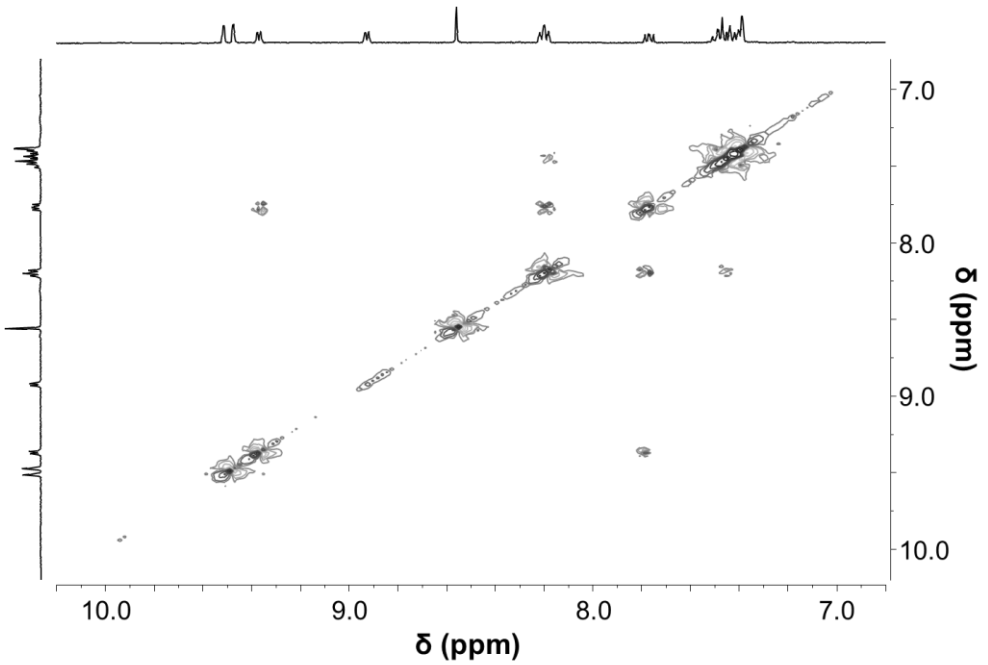


**Figure S18.** $^{1}H$-$^{1}H$ COSY NMR spectrum (400 MHz, DMSO-$d_6$, 298 K) of **1a**.

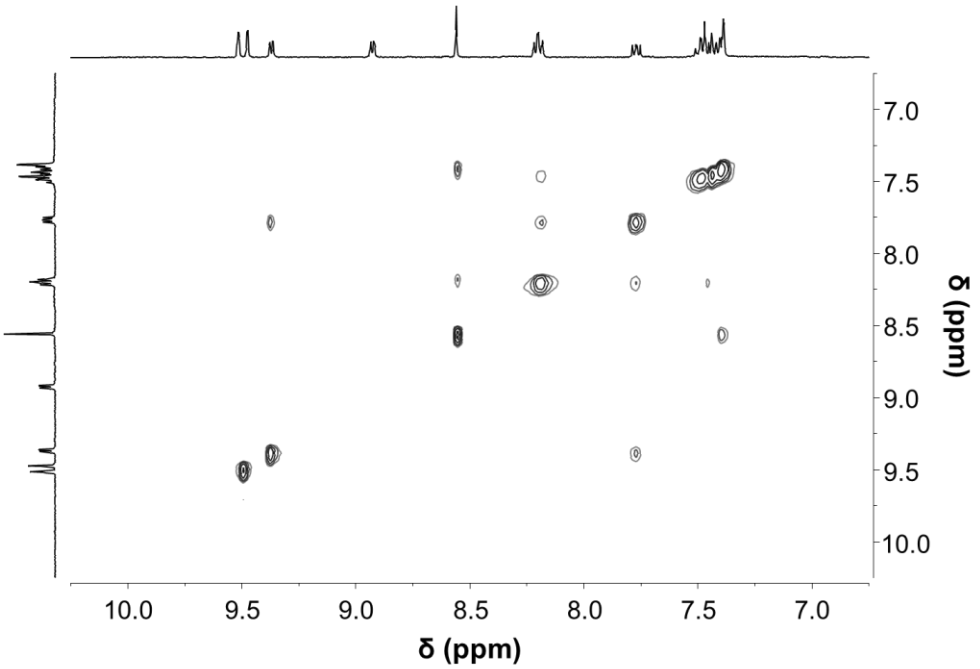


**Figure S19.** NOESY NMR spectrum (400 MHz, DMSO-$d_6$, 298 K) of **1a**.

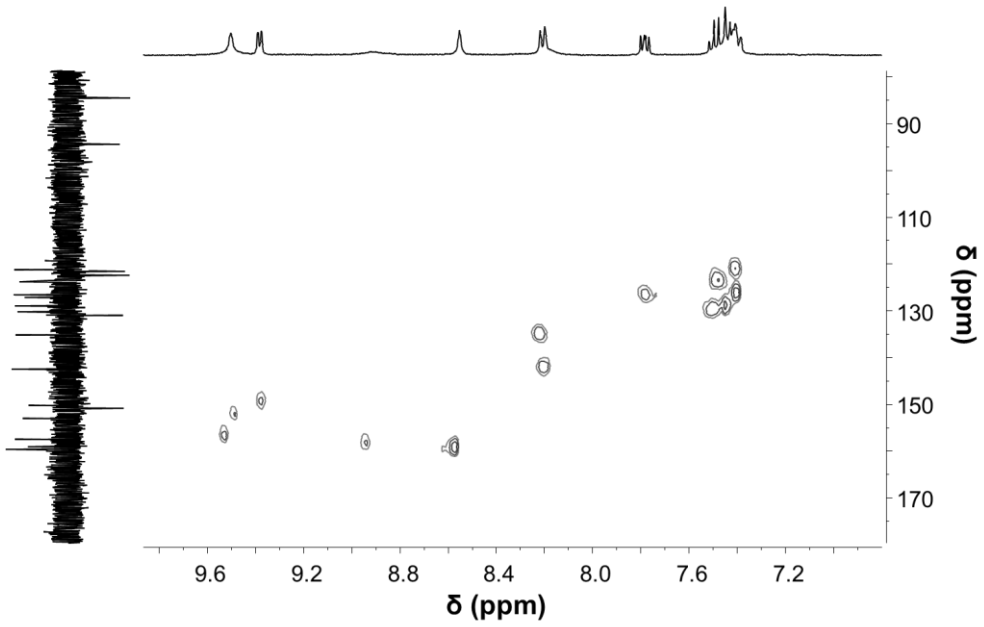


**Figure S20.** HSQC NMR spectrum (400 MHz, DMSO-$d_6$, 298 K) of **1a**.

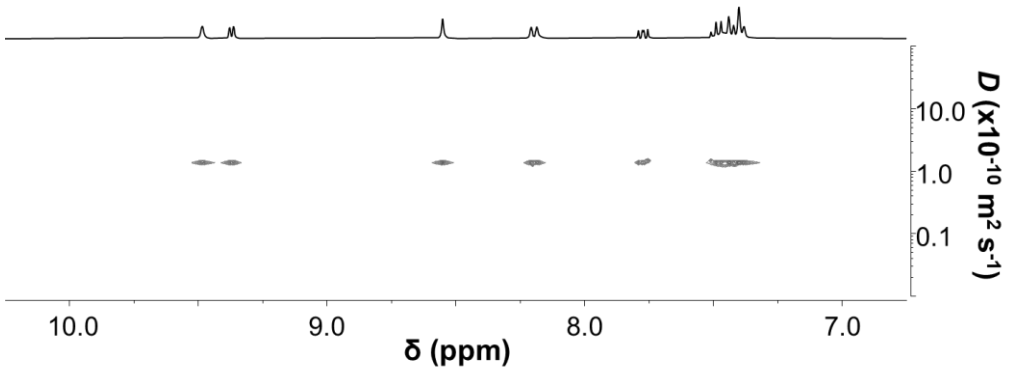


**Figure S21.** DOSY NMR spectrum (400 MHz, DMSO-$d_6$, 298 K) of **1a**.

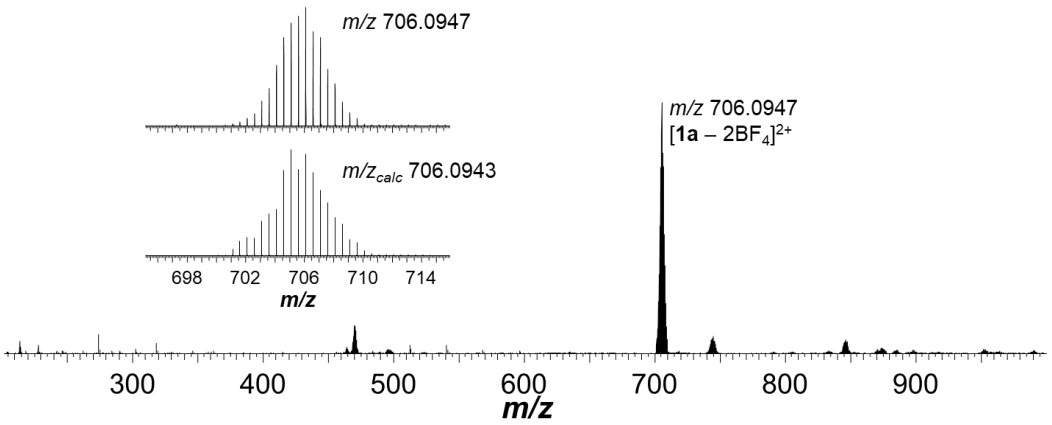


**Figure S22.** ESI-mass spectrum (DMSO/MeCN) of **1a**.

Synthesis of **2a**

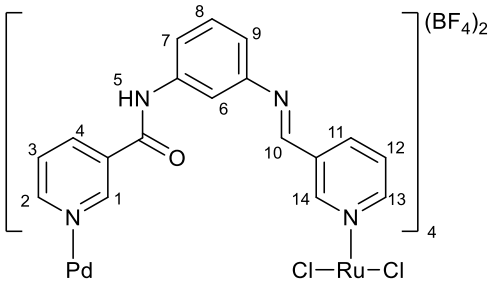


Complex **2a** was prepared analogously to **1a** using compound **2** (75 mg, 0.352 mmol), $[Pd(MeCN)_4](BF_4)_2$ (39 mg, 0.088 mmol), and $[Ru(3\text{-}PA)_4Cl_2]$ **a** (53 mg, 0.088 mmol) to yield an orange solid (124 mg, 84%). Single crystals suitable for X-ray diffraction were grown *via* vapour diffusion of EtOAc into a solution of **2a** in DMSO. $^1$H NMR (400 MHz, DMSO-$d_6$, 298K) δ 10.68 (s, 4H, H-5), 10.40 (d, *J* = 1.4 Hz, 4H, H-1), 9.34 (d, *J* = 5.4 Hz, 4H, H-2), 9.20 (s, 4H, H-14), 8.99 (d, *J* = 5.4 Hz, 4H, H-13), 8.63 (d, *J* = 7.9 Hz, 4H, H-4), 8.55 (s, 4H, H-10), 8.30 (d, *J* = 8.0 Hz, 4H, H-11), 8.19 (t, *J* = 1.8 Hz, 4H, H-6), 7.86 (dd, *J* = 8.0, 5.8 Hz, 4H, H-3), 7.45 (dd, *J* = 7.6, 6.0 Hz, 4H, H-12), 7.37 (t, *J* = 7.9 Hz, 4H, H-8), 7.14 (dd, *J* = 8.1, 1.1 Hz, 4H, H-7), 7.07 – 7.01 (m, 4H, H-9) ppm. $^{13}$C{$^1$H} DEPTQ NMR (126 MHz, DMSO-$d_6$, 298 K) δ 162.0 (Cq × 2), 160.0 (C-10, 13 & 14), 153.5 (C-2), 153.1 (C-1), 152.5 (Cq), 139.5 (Cq), 138.6 (C-4), 133.5 (Cq), 132.8 (C-11), 129.8 (C-8), 127.0 (C-3), 124.3 (C-12) 118.9 (C-9), 118.2 (C-7), 112.7 (C-6) ppm. ESI-MS: *m/z* 744.1064 ($[M - 2BF_4]^{2+}$ $m/z_{calc}$ 744.1060).

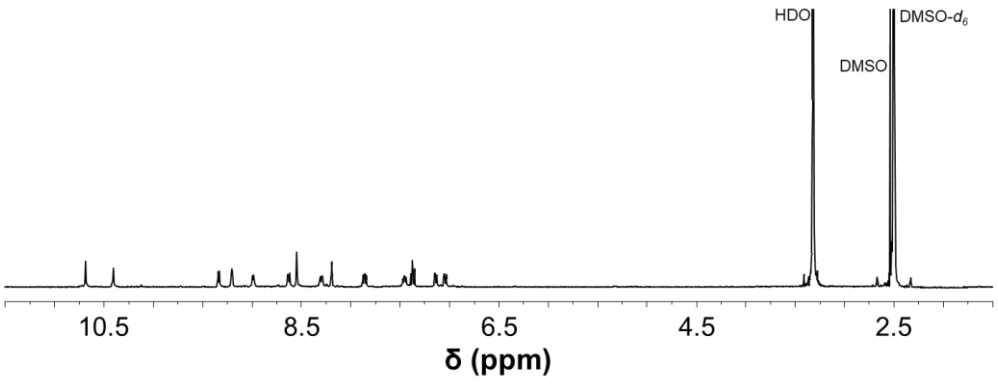


**Figure S23.** $^1$H NMR spectrum (400 MHz, DMSO-$d_6$, 298 K) of **2a**.

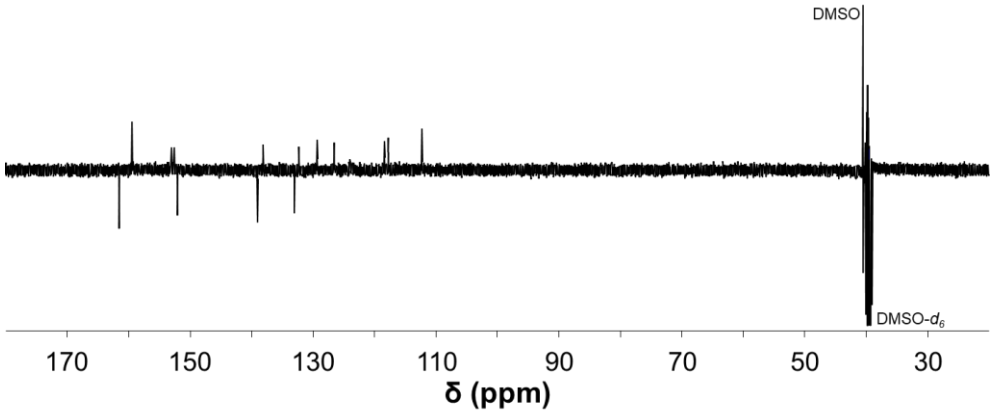


**Figure S24.** $^{13}C\{^{1}H\}$-DEPTQ NMR spectrum (126 MHz, DMSO-$d_6$, 298 K) of **2a**.

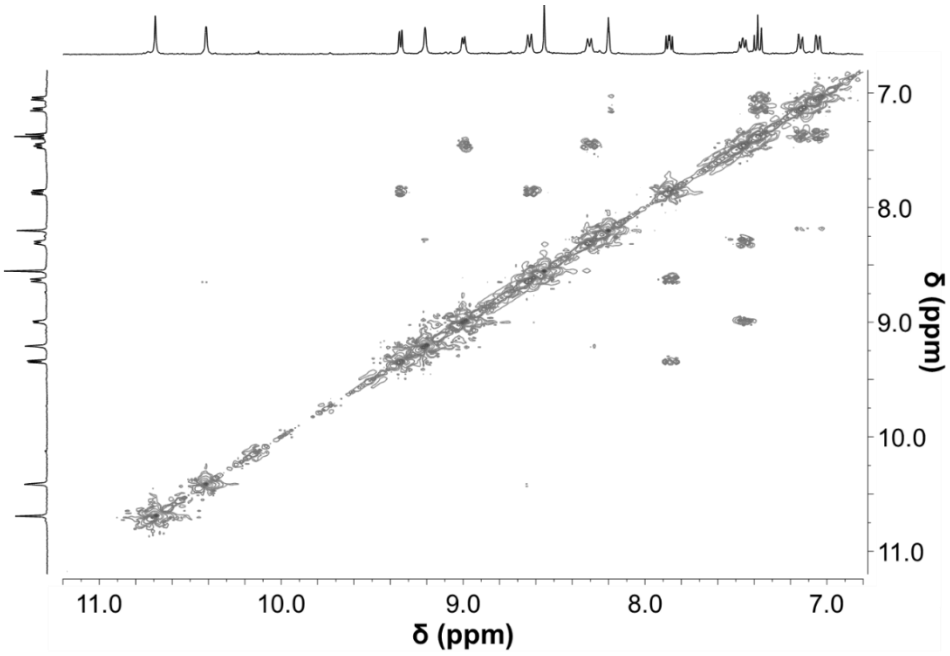


**Figure S25.** $^{1}H$-$^{1}H$ COSY NMR spectrum (400 MHz, DMSO-$d_6$, 298 K) of **2a**.

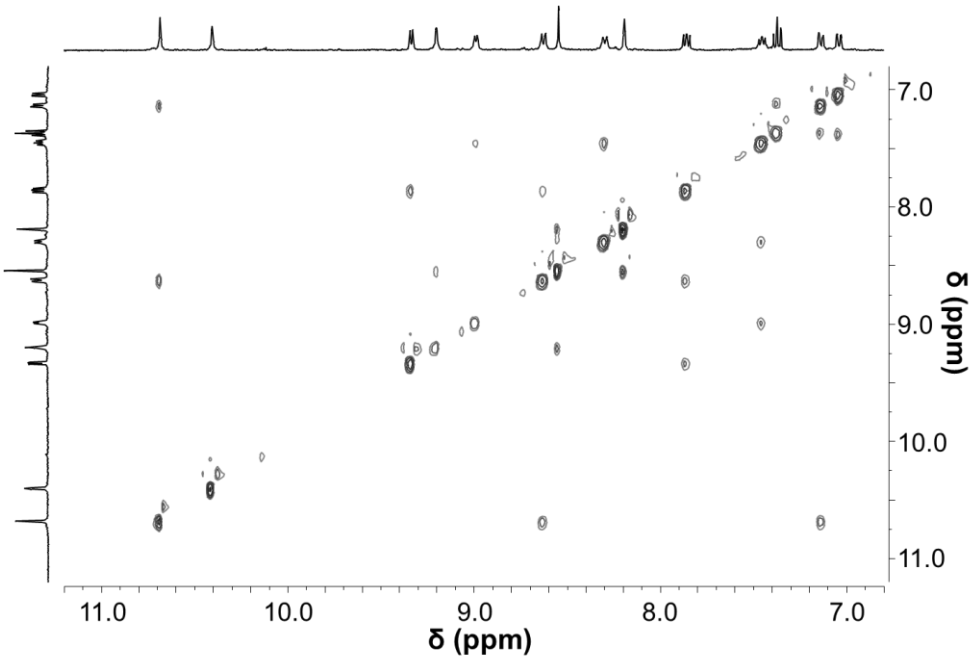


**Figure S26.** NOESY NMR spectrum (400 MHz, DMSO-$d_6$, 298 K) of **2a**.

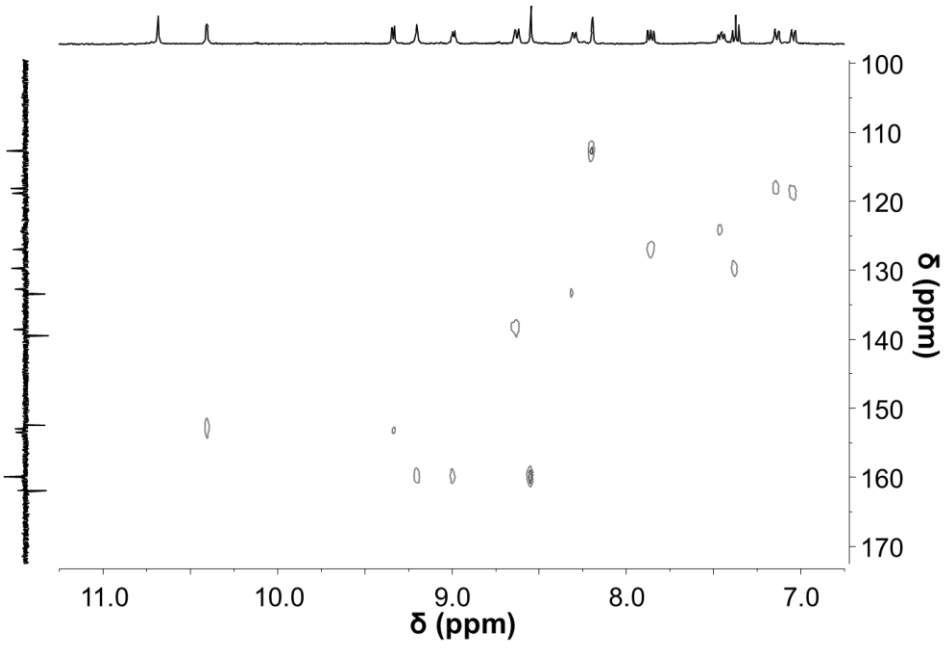


**Figure S27.** HSQC NMR spectrum (400 MHz, DMSO-$d_6$, 298 K) of **2a**.

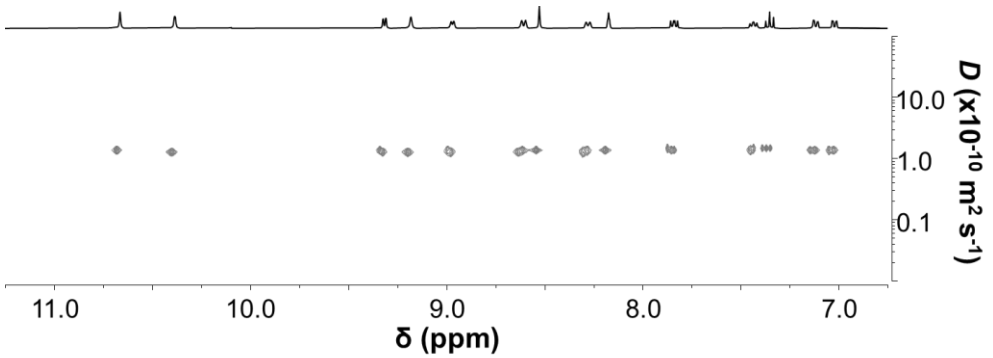


**Figure S28.** DOSY NMR spectrum (400 MHz, DMSO-$d_6$, 298 K) of **2a**.

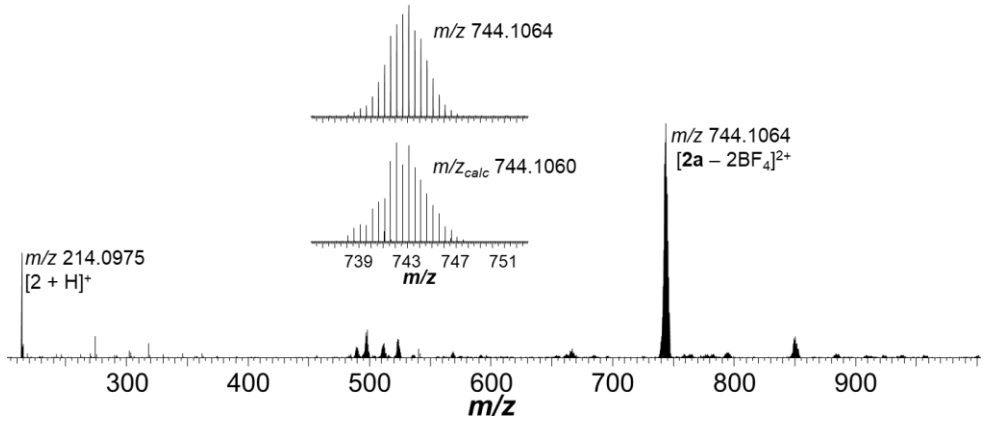


**Figure S29.** ESI-mass spectrum (DMSO/MeCN) of **2a**.

Synthesis of **3a**

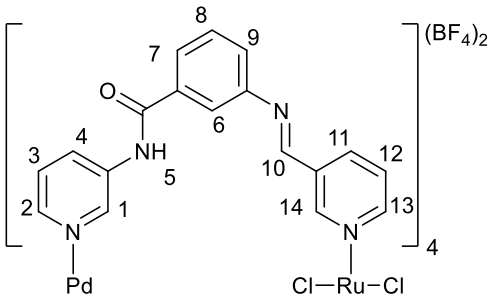


Complex **3a** was prepared analogously to **1a** using compound **3** (75 mg, 0.352 mmol), $[Pd(MeCN)_4](BF_4)_2$ (39 mg, 0.088 mmol), and $[Ru(3\text{-}PA)_4Cl_2]$ **a** (53 mg, 0.088 mmol) to yield a red solid (124 mg, 84%). Single crystals of suitable quality for X-ray diffraction analysis were grown *via* vapour diffusion of EtOAc into a solution of **3a** in DMF. $^1$H NMR (400 MHz, DMSO-$d_6$, 298 K) δ 10.92 (s, 4H, H-5), 9.37 (s, 4H, H-14), 9.19 (d, *J* = 2.2 Hz, 4H, H-1), 8.93 (ddd, *J* = 8.6, 2.2, 1.2 Hz, 4H, H-4), 8.83 (d, *J* = 5.5 Hz, 4H, H-13), 8.79 – 8.74 (m, 4H, H-2), 8.66 (s, 4H, H-10), 8.24 (d, *J* = 7.9 Hz, 4H, H-11), 7.83 (t, *J* = 1.8 Hz, 4H, H-6), 7.77 (dt, *J* = 6.9, 1.9 Hz, 4H, H-7), 7.68 (dd, *J* = 8.6, 5.7 Hz, 4H, H-3), 7.65 – 7.55 (m, 8H, H-8 & H-9), 7.51 (dd, *J* = 7.5, 6.1 Hz, 4H, H-12) ppm. $^{13}$C{$^1$H} DEPTQ NMR (126 MHz, DMSO-$d_6$, 298 K) δ 165.4 (Cq), 160.0( C-10), 159.3 (C-13), 155.9 (C-14), 150.3 (Cq), 145.9 (C-2), 143.0 (C-1), 137.9 (Cq), 137.0 (C-11), 134.3 (Cq), 131.0 (Cq), 130.4 (C-8 & 4), 127.1 (C-3), 126.8 (C-7), 123.9 (C-12), 122.8 (C-9 & 6) ppm. ESI-MS: *m/z* 744.1059 ($[M - 2BF_4]^{2+}$ $m/z_{calc}$ 744.1060), 783.1129 ($[M - 2BF_4 + DMSO]^{2+}$ $m/z_{calc}$ 783.1129).

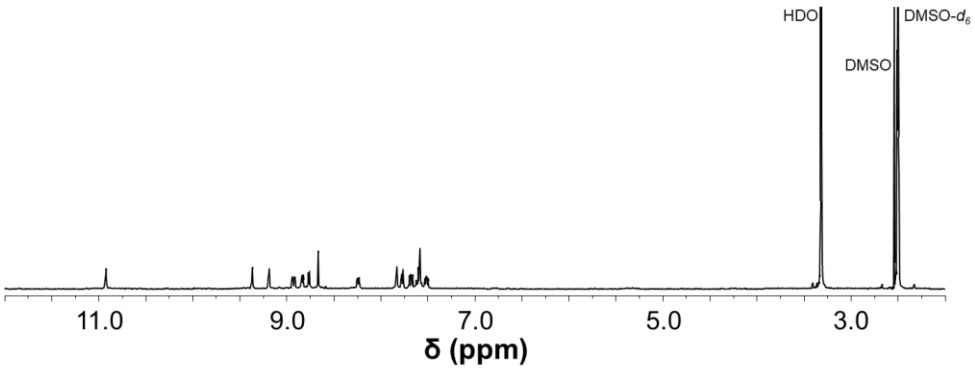


**Figure S30.** $^1$H NMR spectrum (400 MHz, DMSO-$d_6$, 298 K) of **3a**.

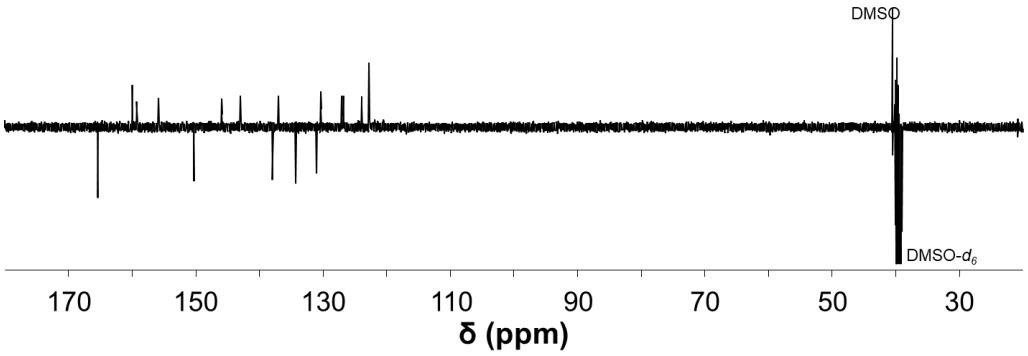


**Figure S31.** $^{13}C\{^{1}H\}$-DEPTQ NMR spectrum (126 MHz, DMSO-$d_6$, 298 K) of **3a**.

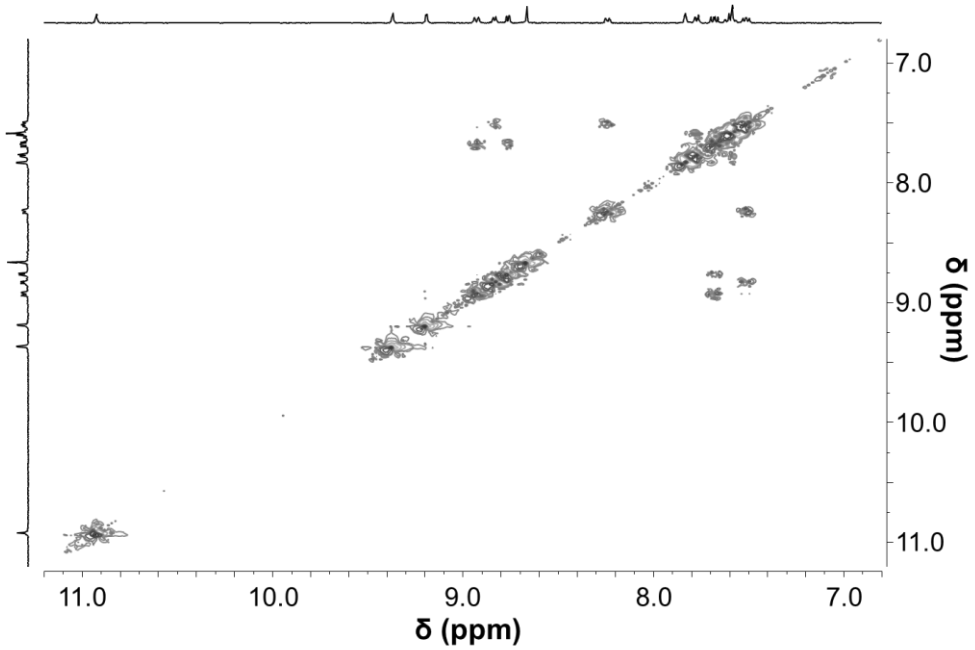


**Figure S32.** $^{1}H$-$^{1}H$ COSY NMR spectrum (400 MHz, DMSO-$d_6$, 298 K) of **3a**.

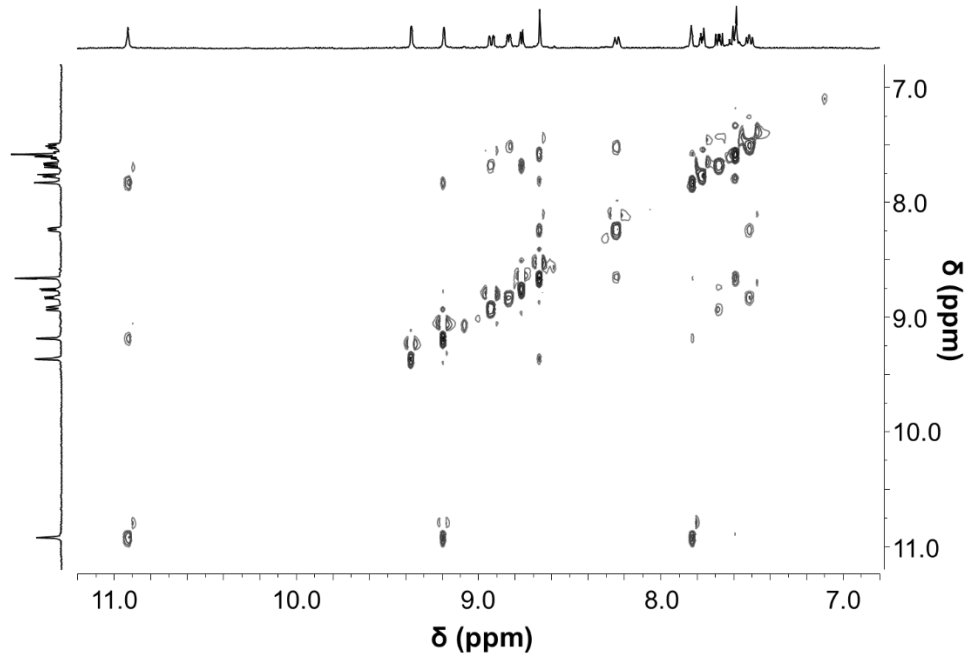


**Figure S33.** NOESY NMR spectrum (400 MHz, DMSO-$d_6$, 298 K) of **3a**.

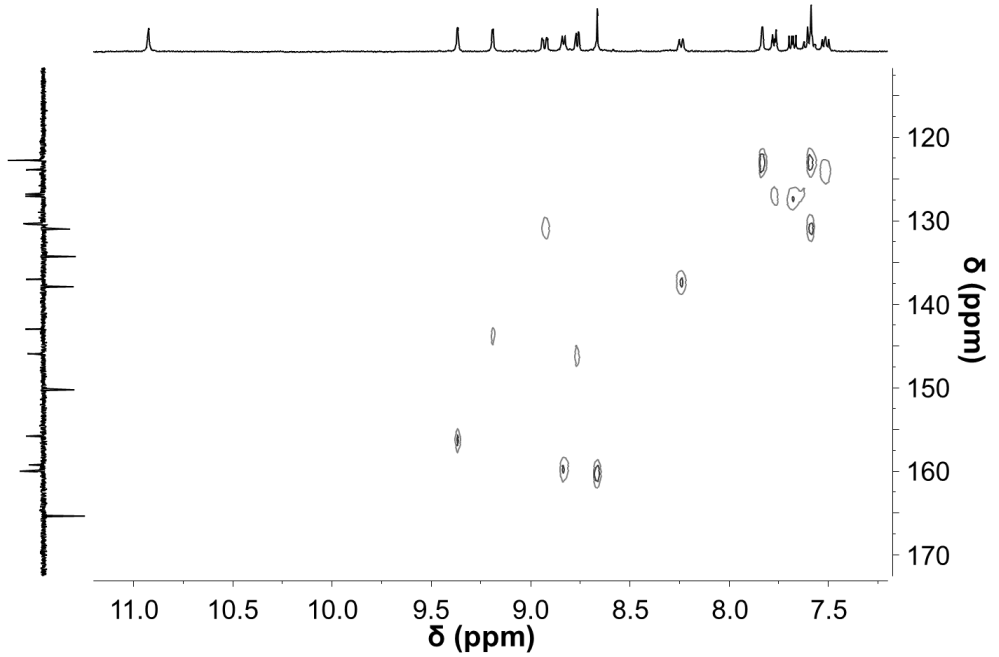


**Figure S34.** HSQC NMR spectrum (400 MHz, DMSO-$d_6$, 298 K) of **3a**.

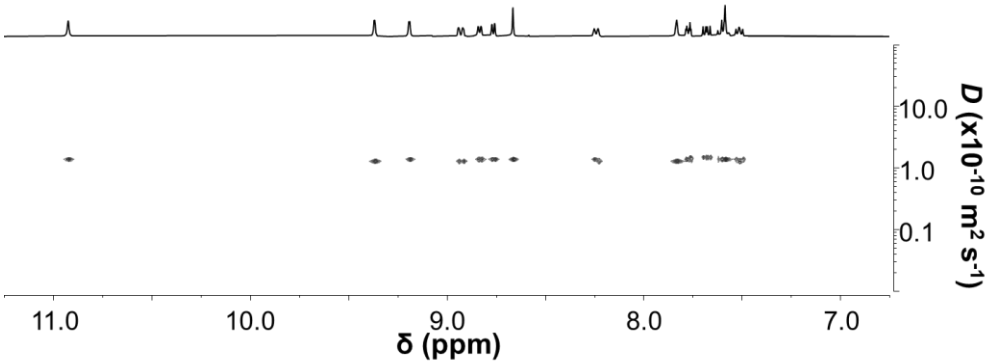


**Figure S35.** DOSY NMR spectrum (400 MHz, DMSO-$d_6$, 298 K) of **3a**.

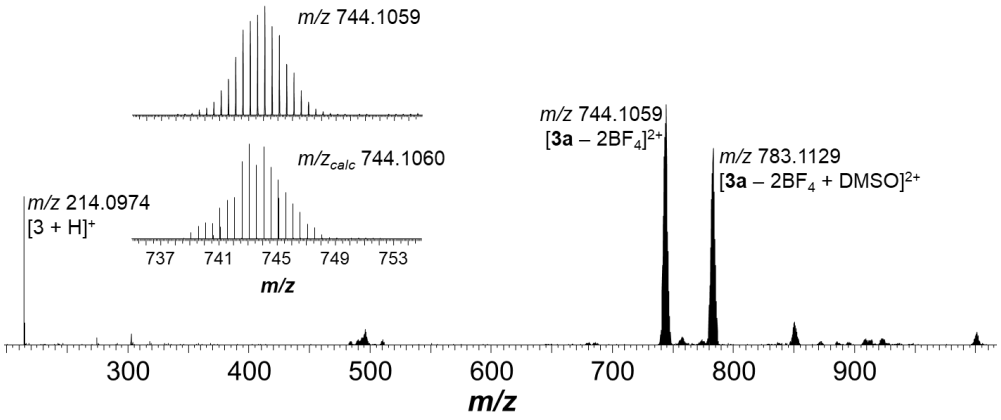


**Figure S36.** ESI-mass spectrum (DMSO/MeCN) of **3a**.

Synthesis of **2b**

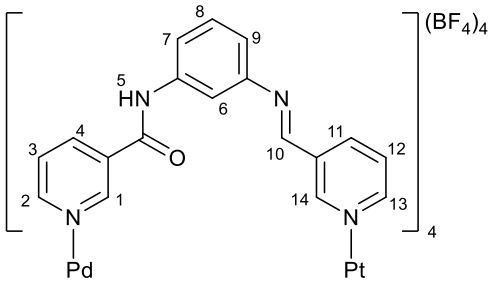


Compound **2** (50 mg, 0.23 mmol), $[Pd(MeCN)_4](BF_4)_2$ (26 mg, 0.059 mmol), and $[Pt(3\text{-}PA)_4](BF_4)_2$ **b** (47 mg, 0.059 mmol) were added to DMSO (2.5 mL) and stirred for 1 h. After addition of EtOAc (ca. 40 mL), the precipitate was filtered, washed with EtOAC (10 mL), $Et_2O$ (10 mL) and DCM (10 mL) to give **2b** as an off white powder (100 mg, 92%). Single crystals suitable for X-ray diffraction were grown *via* vapour diffusion of EtOAc into a solution of **2b** in DMSO. $^1$H NMR (400 MHz, DMSO-$d_6$, 298 K) δ 10.72 (s, 4H, H-5), 10.56 (d, *J* = 1.7 Hz, 4H, H-1), 9.41 (dd, *J* = 6.0, 0.9 Hz, 4H, H-2), 9.23 (d, *J* = 0.6 Hz, 4H, H-14), 9.18 (dd, *J* = 5.8, 0.9 Hz, 4H, H-13), 9.00 (s, 4H, H-10), 8.86 (t, *J* = 2.0 Hz, 4H, H-6), 8.77 – 8.73 (m, 4H, H-4), 8.71 (dt, *J* = 8.1, 1.4 Hz, 4H, H-11), 7.92 (dd, *J* = 8.0, 5.8 Hz, 4H, H-3), 7.88 (dd, *J* = 8.0, 5.8 Hz, 4H, H-12), 7.43 (t, *J* = 7.9 Hz, 4H, H-8), 7.24 (d, *J* = 8.9 Hz, 4H, H-7), 7.16 (dd, *J* = 7.7, 1.2 Hz, 4H, H-9) ppm. $^{13}$C{$^1$H} DEPTQ NMR (126 MHz, DMSO-$d_6$, 298 Kf) δ 161.4 (Cq), 157.2 (C-10), 155.5 (C-14), 153.8 (C-13), 153.2 (C-2), 152.4 (C-1), 150.1 (Cq), 139.6 (Cq), 138.1 (C-4), 137.3 (C-11), 134.8 (Cq), 132.8 (Cq), 129.8 (C-8), 128.2 (C-12), 126.8 (C-3), 121.4 (C-9), 118.9 (C-7), 109.7 (C-6) ppm. ESI-MS: *m/z* 377.3339 ($[M - 4BF_4]^{4+}$ $m/z_{calc}$ 377.3333)

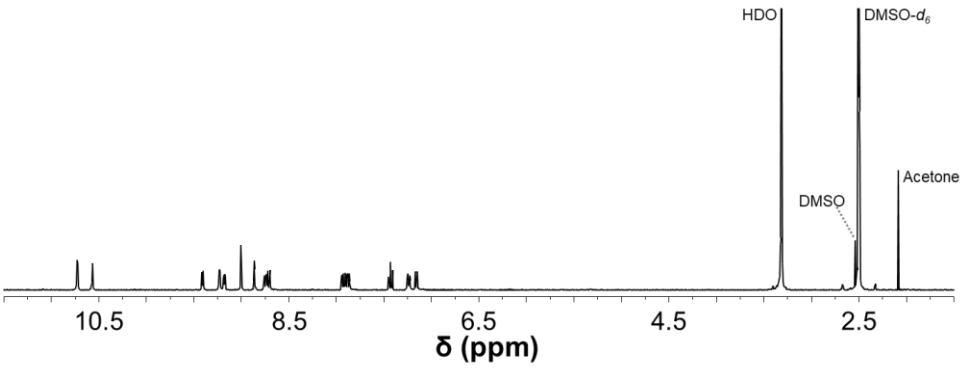


**Figure S37.** $^1$H NMR spectrum (400 MHz, DMSO-$d_6$, 298 K) of **2b**.

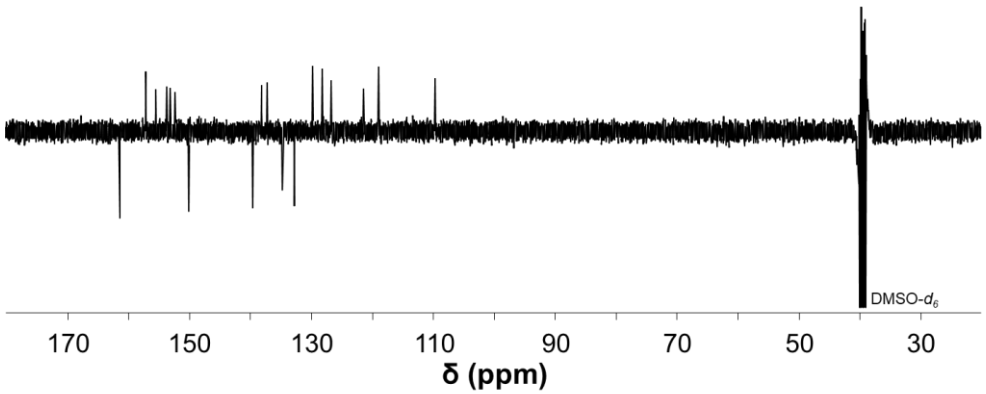


**Figure S38.** $^{13}C\{^{1}H\}$-DEPTQ NMR spectrum (126 MHz, DMSO-$d_6$, 298 K) of **2b**.

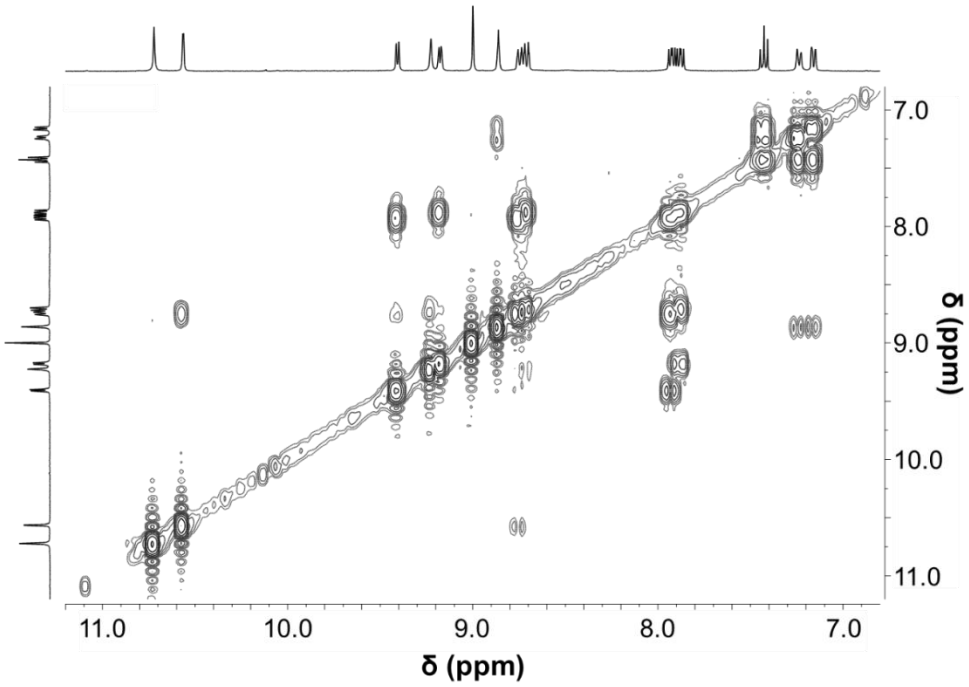


**Figure S39.** $^{1}H$-$^{1}H$ COSY NMR spectrum (400 MHz, DMSO-$d_6$, 298 K) of **2b**.

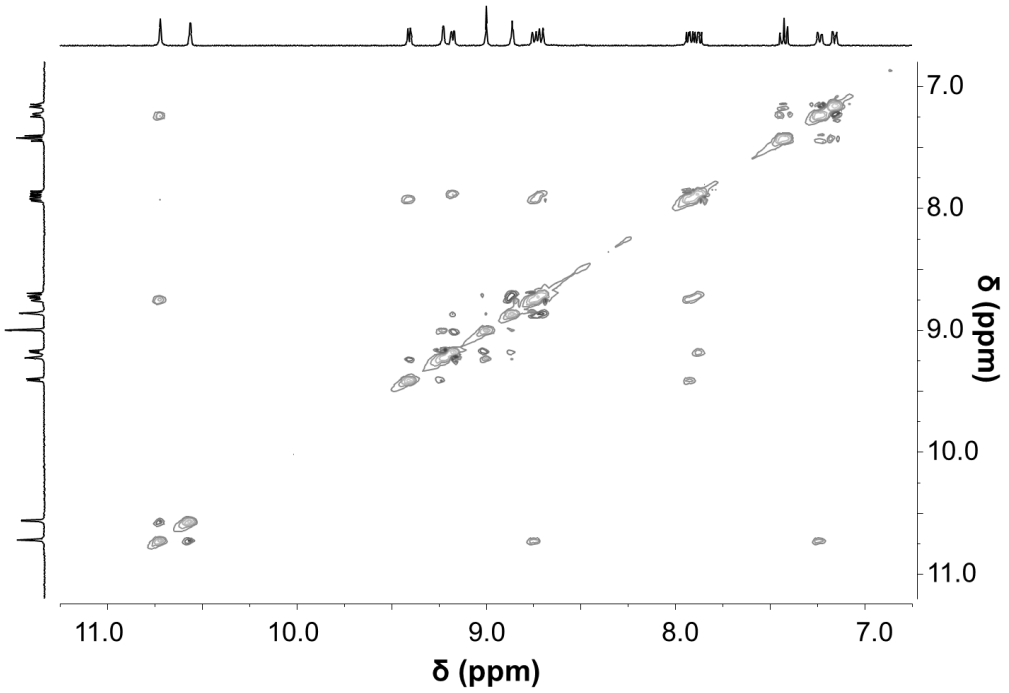


**Figure S40.** NOESY NMR spectrum (400 MHz, DMSO-$d_6$, 298 K) of **2b**.

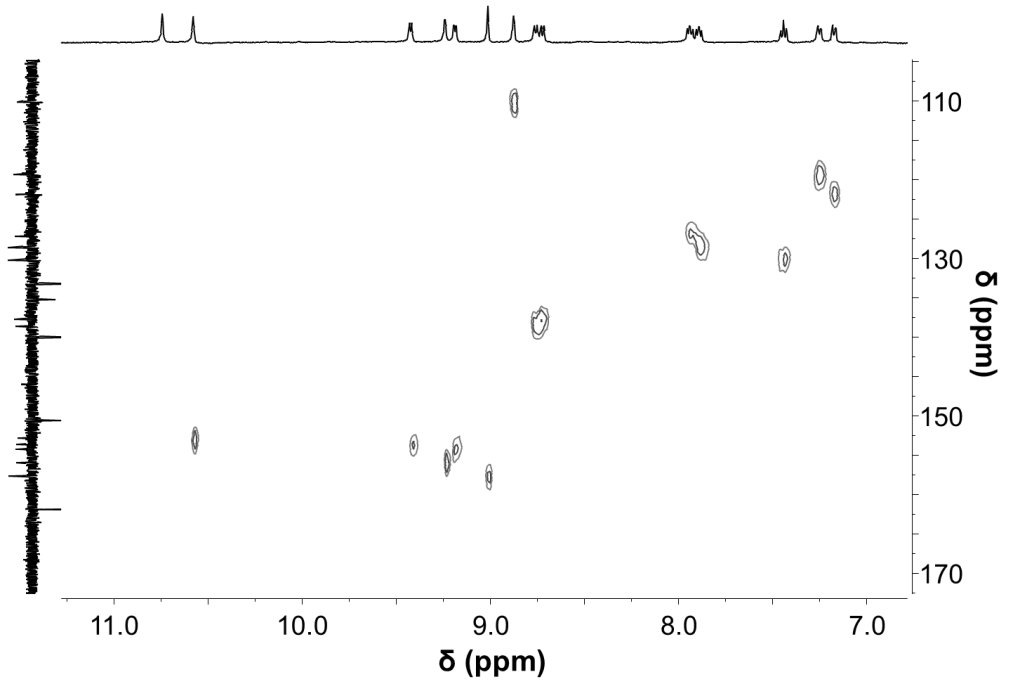


**Figure S41.** HSQC NMR spectrum (400 MHz, DMSO-$d_6$, 298 K) of **2b**.

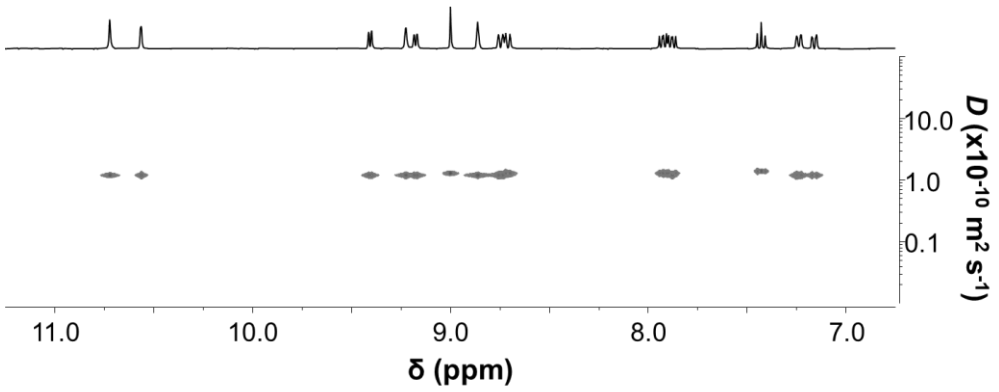


**Figure S42.** DOSY NMR spectrum (400 MHz, DMSO-$d_6$, 298 K) of **2b**.

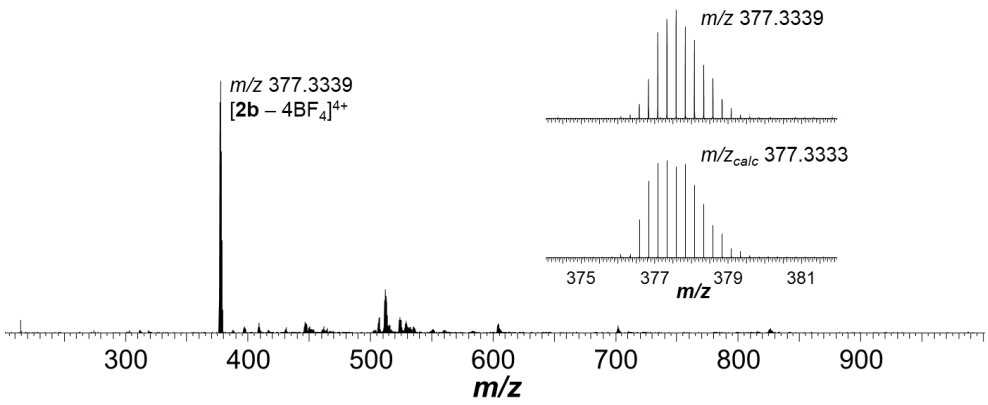


**Figure S43.** ESI-mass spectrum (DMSO/MeCN) of **2b**.

Synthesis of **3b**

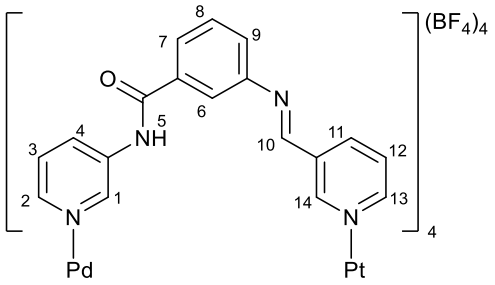


Compound **3** (50 mg, 0.23 mmol), $[Pd(MeCN)_4](BF_4)_2$ (26 mg, 0.059 mmol), and $[Pt(3\text{-}PA)_4](BF_4)_2$ **b** (47 mg, 0.059 mmol) were added to DMSO (2.5 mL) and stirred for 1 h. After addition of EtOAc (ca. 40 mL), the precipitate was filtered, washed with EtOAC (10 mL), $Et_2O$ (10 mL) and DCM (10 mL) to give **3b** as an off-white powder (98 mg, 90%). $^1$H NMR (400 MHz, DMSO-$d_6$, 298 K) δ 10.89 (s, 4H, H-5), 10.39 (d, *J* = 1.1 Hz, 4H, H-1), 10.13 (d, *J* = 0.9 Hz, 4H, H-14), 9.36 (dd, *J* = 5.7, 0.9 Hz, 4H, H-13), 9.11 (dd, *J* = 5.5, 0.8 Hz, 4H, H-2), 9.03 (s, 4H, H-10), 8.50 (dt, *J* = 8.0, 1.5 Hz, 4H, H-11), 8.39 (t, *J* = 1.6 Hz, 4H, H-6), 8.07 (t, *J* = 7.3 Hz, 8H, H-4 & H-7), 7.91 (dd, *J* = 7.8, 5.9 Hz, 4H, H-12), 7.80 (dd, *J* = 8.5, 5.6 Hz, 4H, H-3), 7.72 (dd, *J* = 7.9, 1.3 Hz, 4H, H-9), 7.65 (t, *J* = 7.8 Hz, 4H, H-8) ppm. $^{13}$C{$^1$H} DEPTQ NMR (126 MHz, DMSO-$d_6$, 298 K) δ 165.0 (Cq), 157.1 (C-10), 153.3 (C-13), 152.4 (C-14), 149.2 (Cq), 146.2 (C-2), 140.3 (C-1), 139.6 (C-11), 138.8 (Cq), 135.1 (Cq), 133.9 (Cq), 131.2 (C-4), 129.8 (C-8), 128.0 (C-12), 127.6 (C-3), 126.2 (C-7), 125.4 (C-9), 123.3 (C-6) ppm. ESI-MS: *m/z* 377.3338 ($[M - 4BF_4]^{4+}$ $m/z_{calc}$ 377.3333).

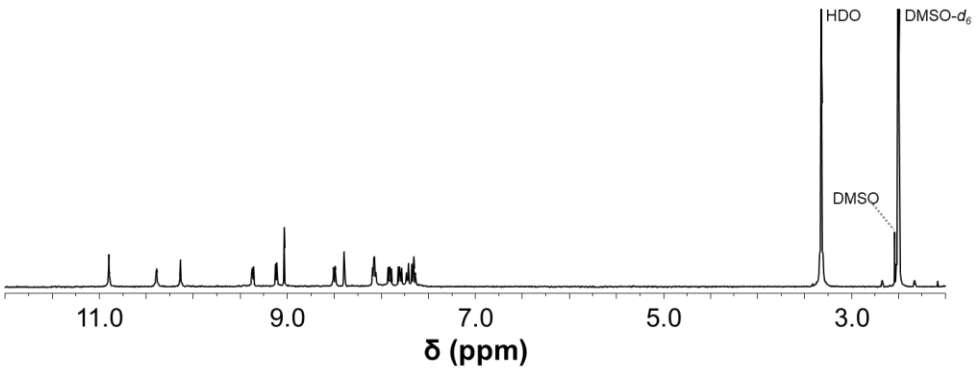


**Figure S44.** $^1$H NMR spectrum (400 MHz, DMSO-$d_6$, 298 K) of **3b**.

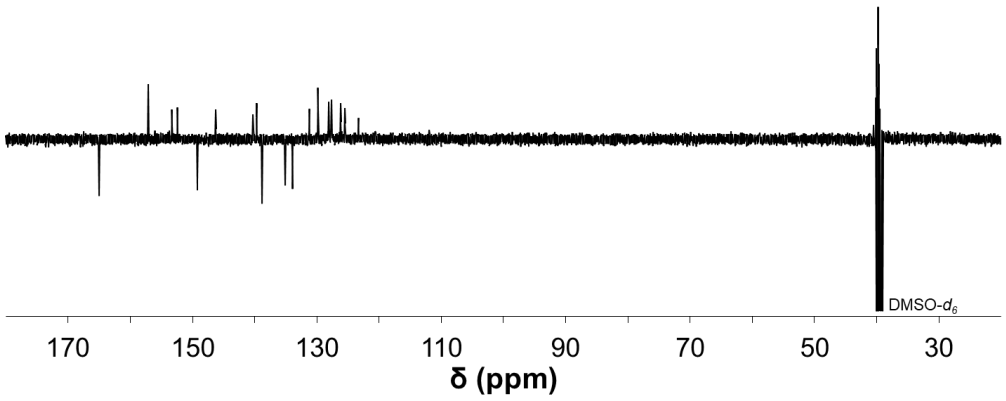


**Figure S45.** $^{13}C\{^1H\}$-DEPTQ NMR spectrum (101 MHz, DMSO-$d_6$, 298 K) of **3b**.

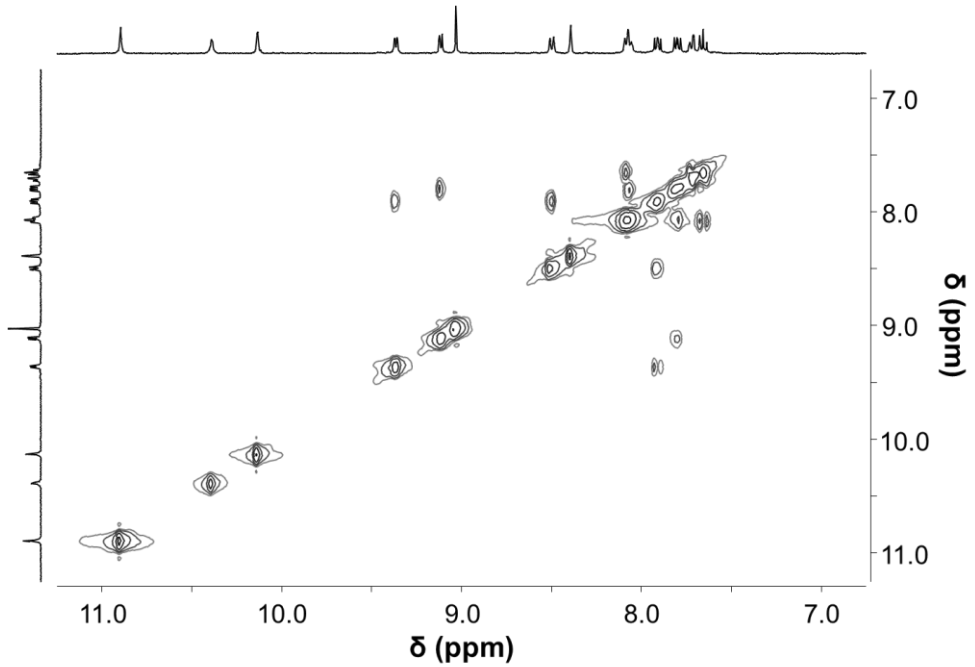


**Figure S46**. $^1H$-$^1H$ COSY spectrum (400 MHz, DMSO-$d_6$, 298 K) of **3b**.

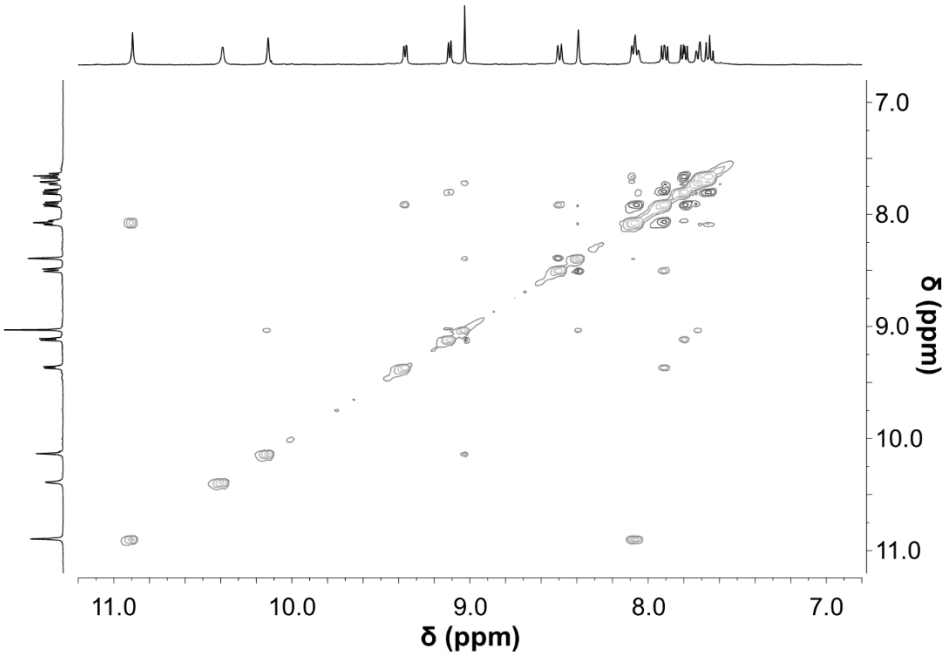


**Figure S47.** NOESY NMR spectrum (400 MHz, DMSO-$d_6$, 298 K) of **3b**.

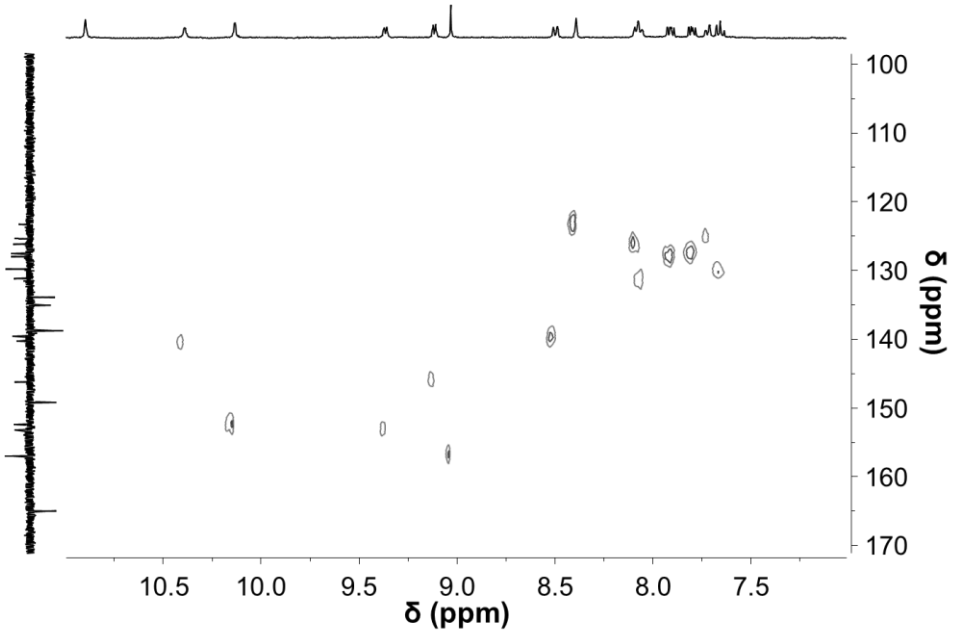


**Figure S48.** HSQC NMR spectrum (400 MHz, DMSO-$d_6$, 298 K) of **3b**.

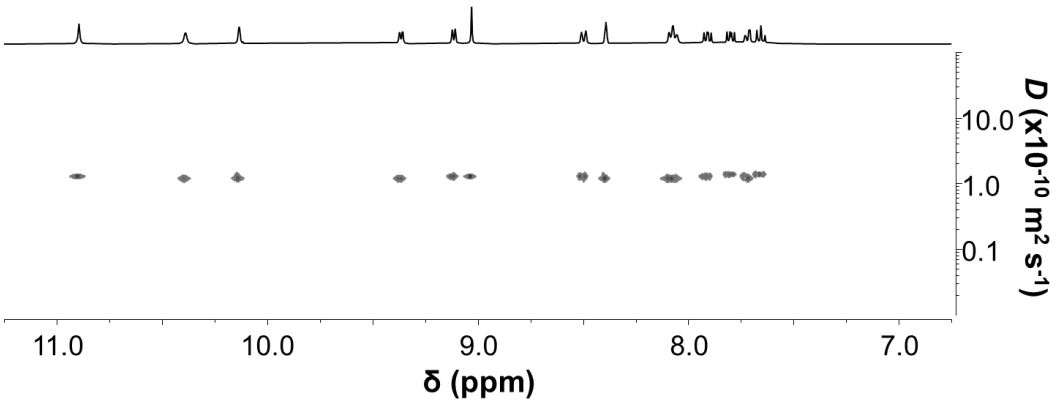


**Figure S49.** DOSY NMR spectrum (400 MHz, DMSO-$d_6$, 298 K) of **3b**.

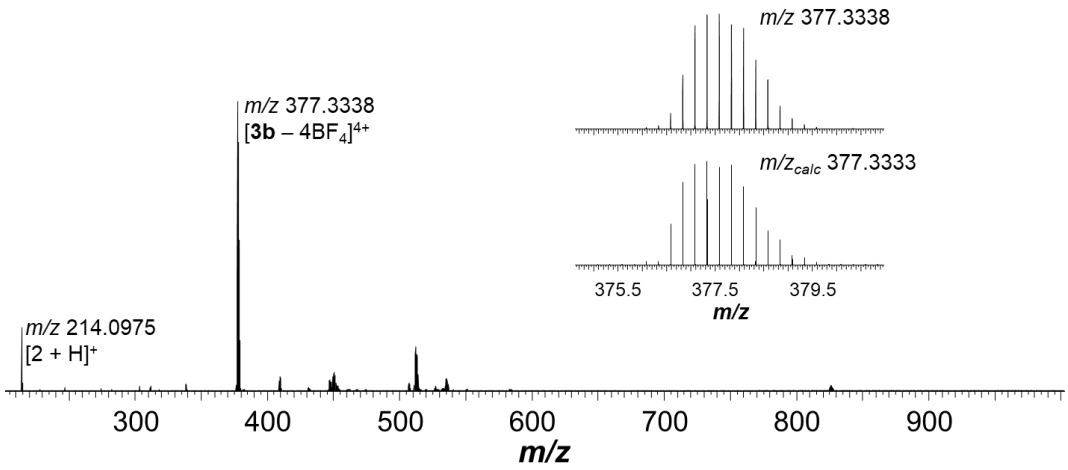


**Figure S50.** ESI-mass spectrum (DMSO/MeCN) of **3b**.

## Diffusion coefficient determination

Diffusion coefficients of compounds **1a**–**3b** were obtained *via* $^{1}$H diffusion ordered spectroscopy (DOSY) NMR experiments.

**Table S1.** Diffusion coefficients as obtained *via* $^{1}$H DOSY NMR experiments (400 MHz, DMSO-$d_6$, 298 K) in comparison to that of **1b**.[2]

| Compound | Molecular weight (g mol$^{-1}$) | Diffusion coefficient (× 10$^{-10}$ m$^2$ s$^{-1}$) |
|---|---|---|
| **1a** | 1585.33 | 1.34 |
| **2a** | 1661.35 | 1.31 |
| **3a** | 1661.35 | 1.31 |
| **1b** [2] | 1743.00 | 1.22 |
| **2b** | 1858.07 | 1.25 |
| **3b** | 1858.07 | 1.25 |

## Stimulus responsiveness investigations

To assess the abilities of MSAs **1a**–**3b** to open and close in the presence of external stimuli, NMR titrations were carried out with 4-(dimethylamino)pyridine (DMAP) to open the cage and *p*-toluenesulfonic acid (*p*-TsOH) to close it.

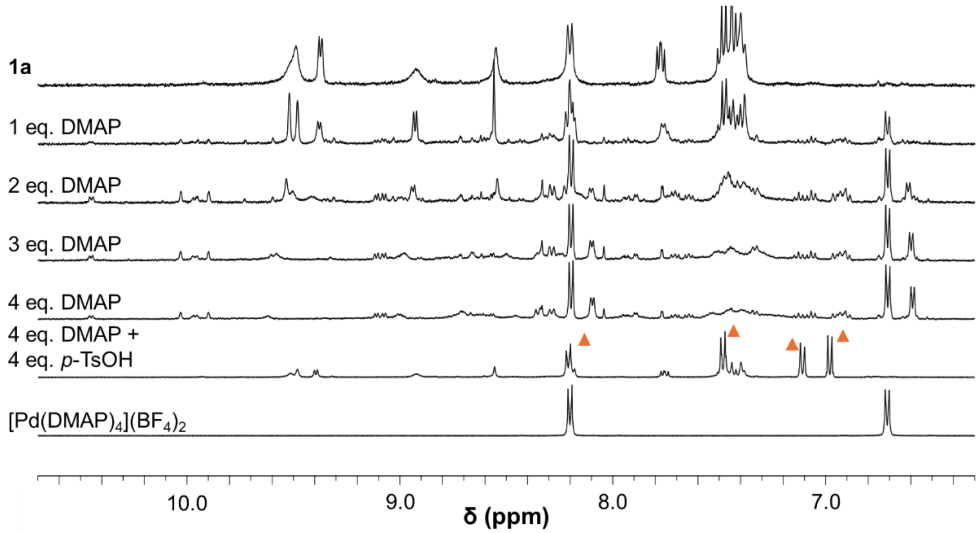


**Figure S51.** $^{1}$H NMR (400 MHz, DMSO-$d_6$, 298 K) spectra of the titration of DMAP into **1a** (2 mM), followed by addition of 4 eq. of *p*-TsOH. Signals labelled with ▲ are attributed to *N*,*N*-dimethylaminopyridinium tosylate. The larger number of signals found after addition of 4 eq. DMAP may be due to a mixture of products formed during the disassembly process or hydrolysis of the Schiff base, which however seem to be reversible by addition of *p*-TsOH.

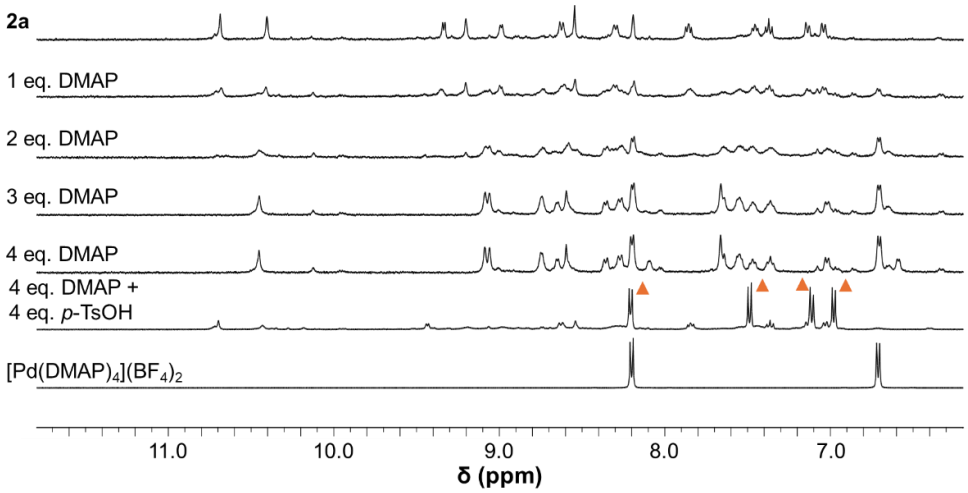


**Figure S52.** $^{1}$H NMR (400 MHz, DMSO-$d_6$, 298 K) spectra of the titration of DMAP into **2a** (2 mM), followed by addition of 4 eq. of *p*-TsOH. Signals labelled with ▲ are attributed to *N*,*N*-dimethylaminopyridinium tosylate.

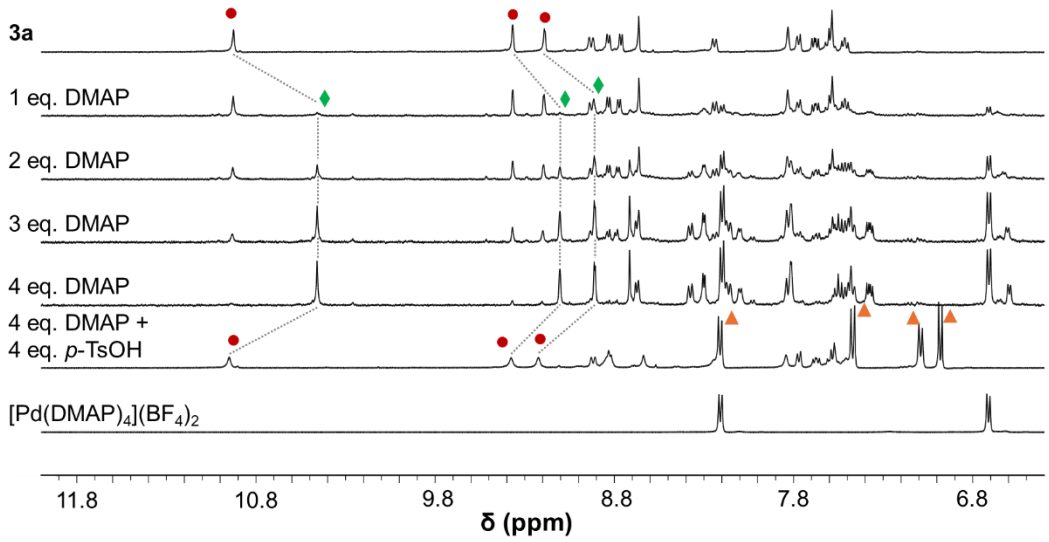


**Figure S53.** $^{1}$H NMR (400 MHz, DMSO-$d_6$, 298 K) spectra of the titration of DMAP into **3a** (2 mM), followed by addition of 4 eq. of *p*-TsOH. Signals labelled with ● are attributed to **3a**, those with ▲ to *N*,*N*-dimethylaminopyridinium tosylate, and ♦ to $[Ru(L)_4Cl_2]$.

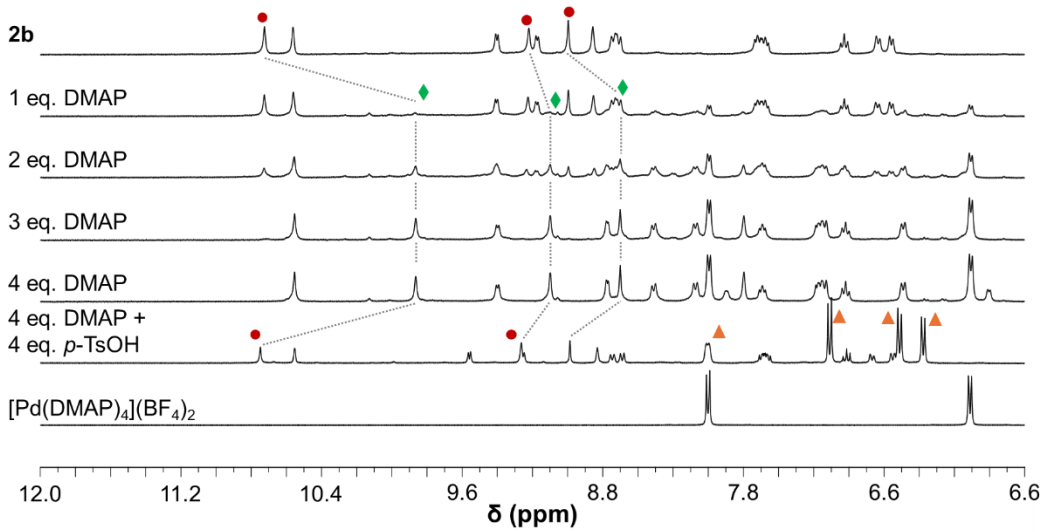


**Figure S54.** $^{1}$H NMR (400 MHz, DMSO-$d_6$, 298 K) spectra of the titration of DMAP into **2b** (2 mM), followed by addition of 4 eq. of *p*-TsOH. Signals labelled with ● are attributed to **2b**, those with ▲ to *N*,*N*-dimethylaminopyridinium tosylate, and ♦ to $[Pt(L)_4]^{2+}$.

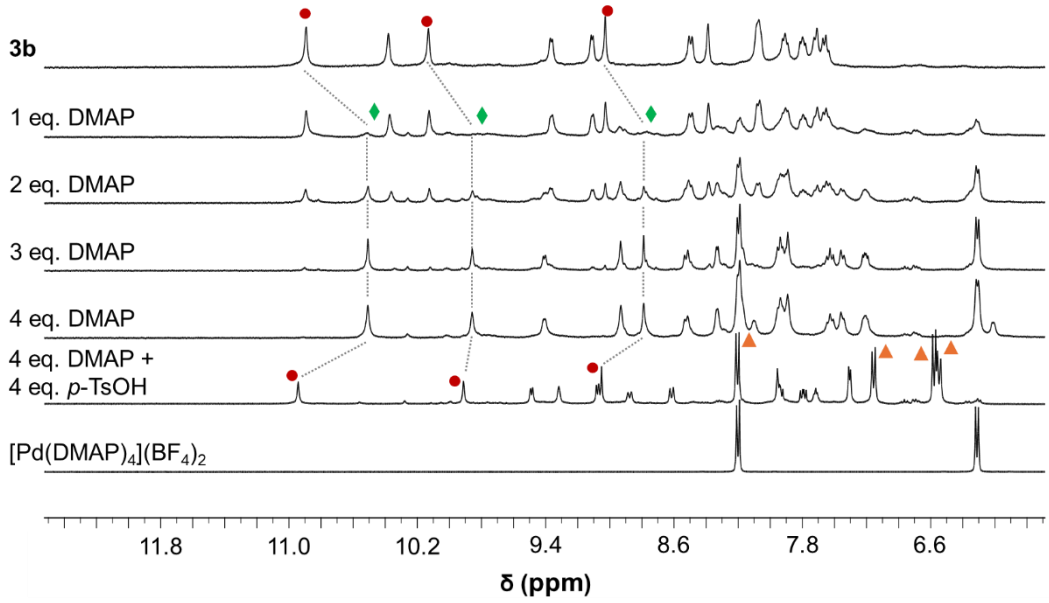


**Figure S55.** $^{1}$H NMR (400 MHz, DMSO-$d_6$, 298 K) spectra of the titration of DMAP into **3b** (2 mM), followed by addition of 4 eq. of *p*-TsOH. Signals labelled with ● are attributed to **3b**, those with ▲ to *N*,*N*-dimethylaminopyridinium tosylate, and ♦ to $[Pt(L)_4]^{2+}$.

## Guest binding studies

All titrations were conducted with host concentrations of 2 mM, and guest concentrations of 100 mM to achieve 0.1 eq./µL concentrations. The lowest addition of guest was 0.2 eq. for sodium mesylate and 0.5 eq. for sodium tosylate. $^{1}$H NMR spectra were recorded immediately after addition of an equivalent and shaking the sample. The binding constants were calculated using Bindfit on http://supramolecular.org.[13] For binding where changes in δ plateaued after addition of 2 equivalents of guest, a 1:2 H:G curve fitting was used whereas for all others a 1:1 curve fitting was used.

## Mesylate binding studies

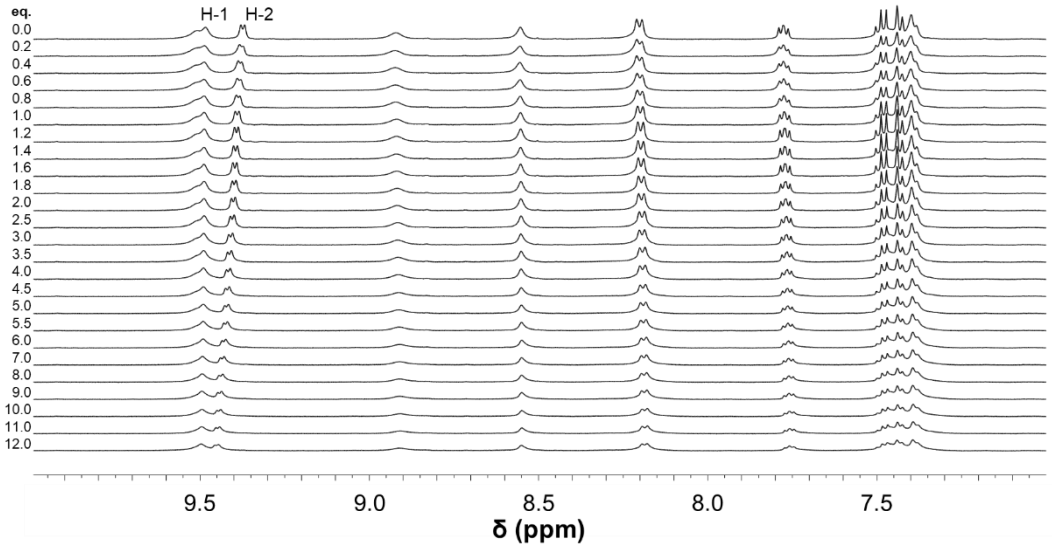


**Figure S56.** $^{1}$H NMR (400 MHz, DMSO-$d_6$, 298 K) spectra for the titration of MsONa into **1a** (2 mM).

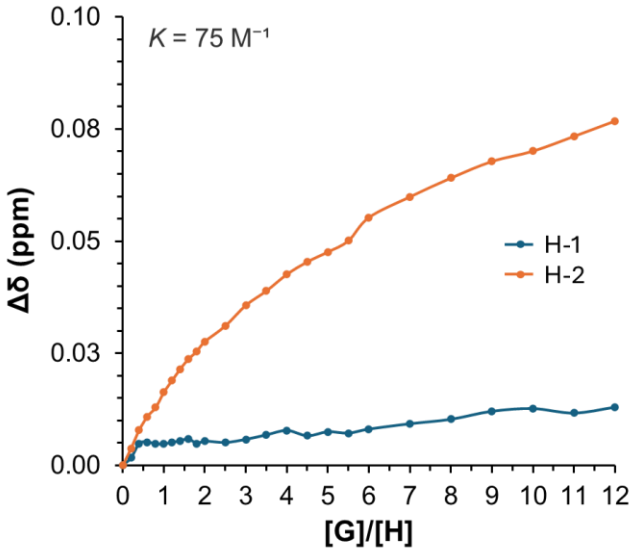


**Figure S57.** Changes in chemical shifts of H-1 and H-2 in the $^{1}$H NMR (400 MHz, DMSO-$d_6$, 298 K) spectra of **1a** (2 mM) after titration with MsONa.

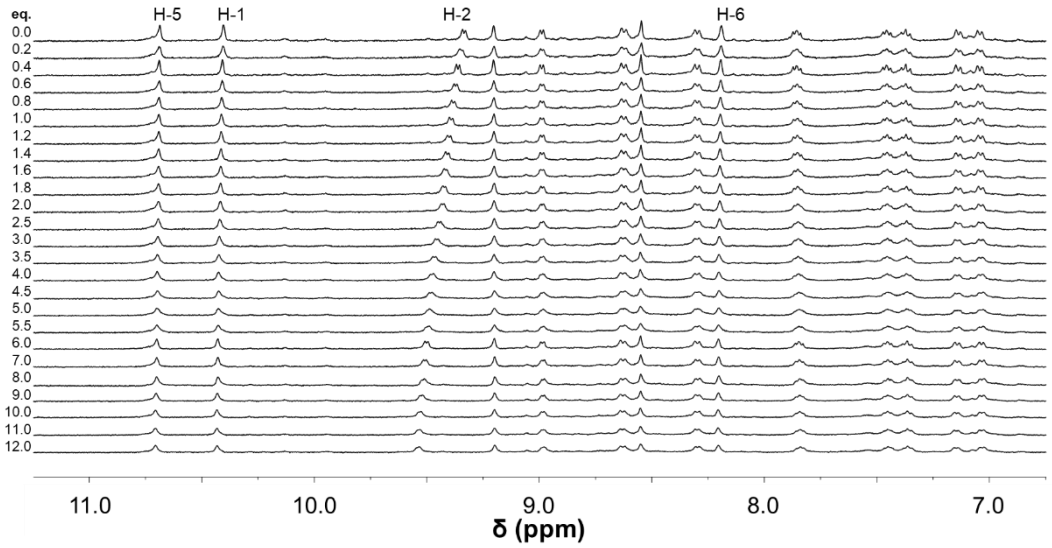


**Figure S58.** $^{1}$H NMR (400 MHz, DMSO-$d_6$, 298 K) spectra for the titration of MsONa into **2a** (2 mM).

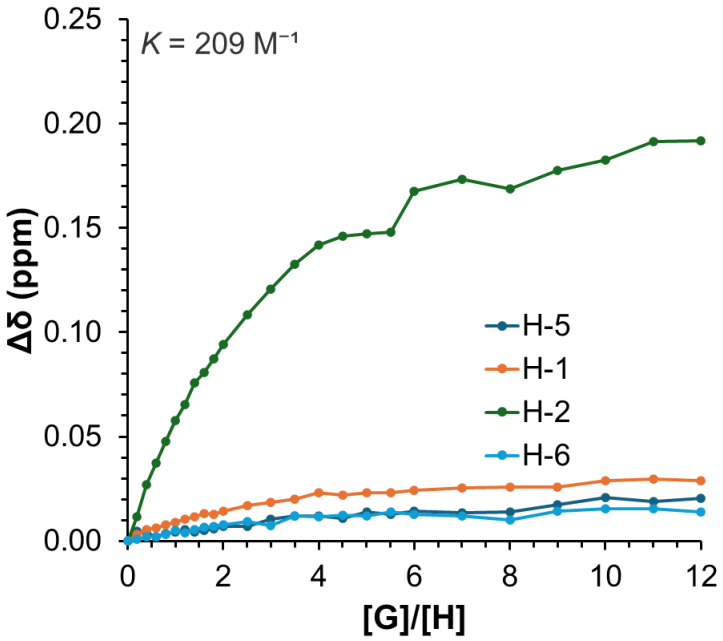


**Figure S59.** Changes in chemical shifts of H-1, H-2, H-5 and H-6 in the $^{1}$H NMR (400 MHz, DMSO-$d_6$, 298 K) spectra of **2a** (2 mM) after titration with MsONa.

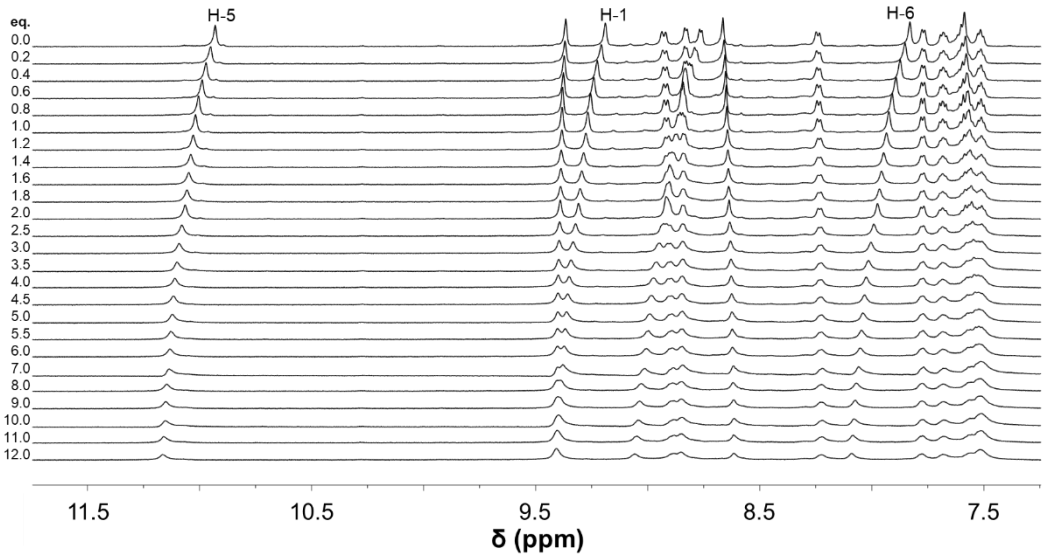


**Figure S60.** $^{1}$H NMR (400 MHz, DMSO-$d_6$, 298 K) spectra for the titration of MsONa into **3a** (2 mM).

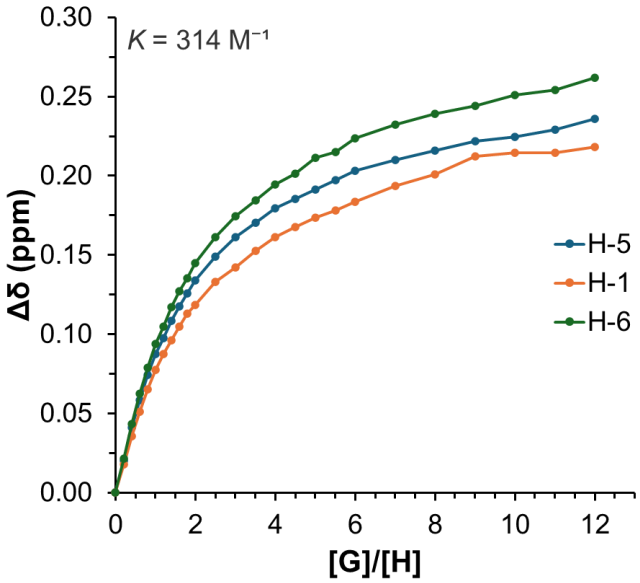


**Figure S61.** Changes in chemical shifts of H-1, H-5 and H-6 in the $^{1}$H NMR (400 MHz, DMSO-$d_6$, 298 K) spectra of **3a** (2 mM) after titration with MsONa.

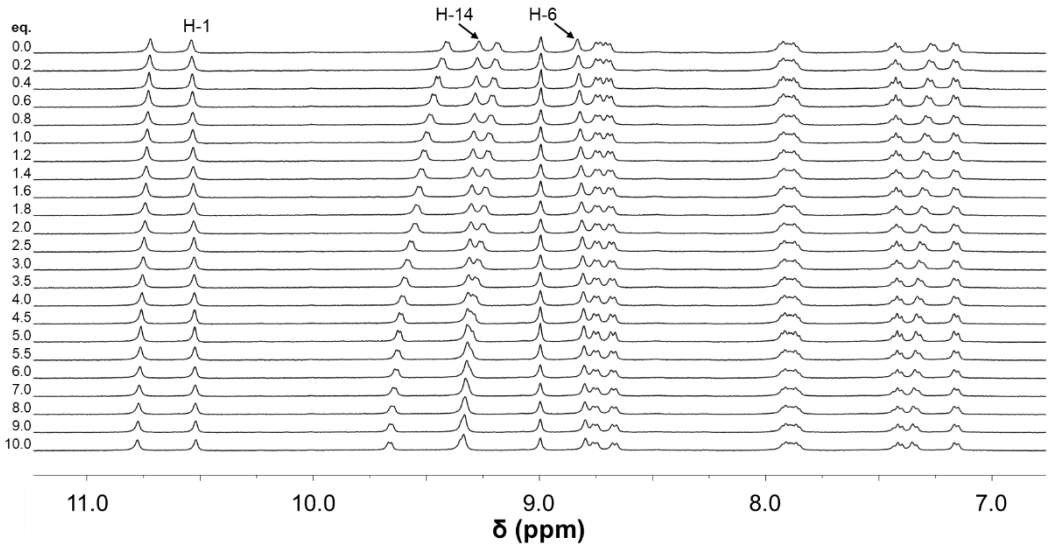


**Figure S62.** $^{1}$H NMR (400 MHz, DMSO-$d_6$, 298 K) spectra for the titration of MsONa into **2b** (2 mM).

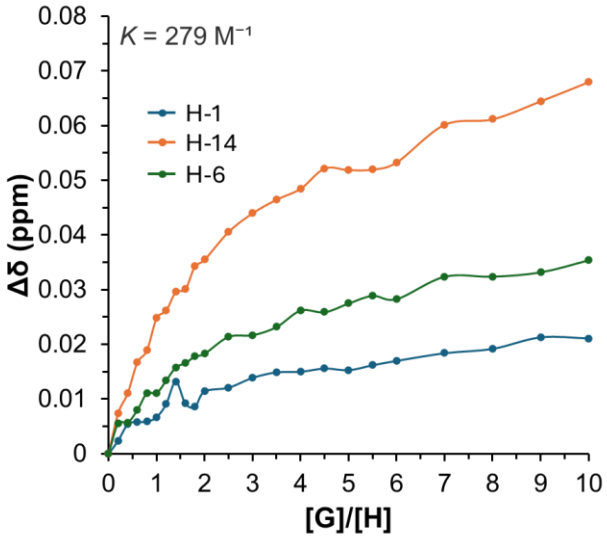


**Figure S63.** Changes in chemical shifts of H-1, H-6 and H-14 in the $^{1}$H NMR (400 MHz, DMSO-$d_6$, 298 K) spectra of **2b** (2 mM) after titration with MsONa.

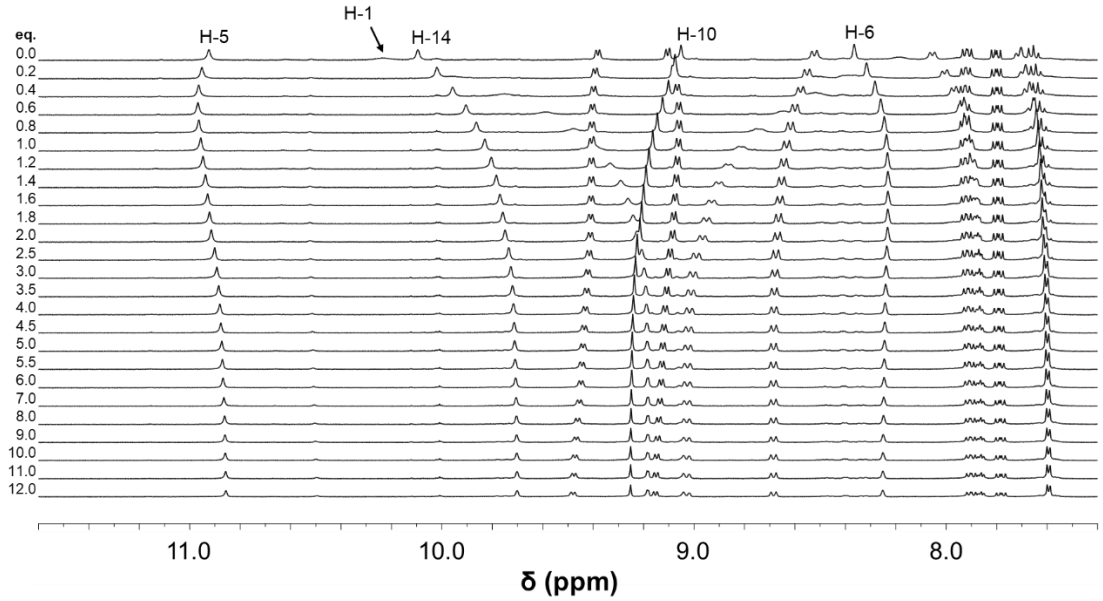


**Figure S64.** $^{1}$H NMR (400 MHz, DMSO-$d_6$, 298 K) spectra for the titration of MsONa into **3b** (2 mM).

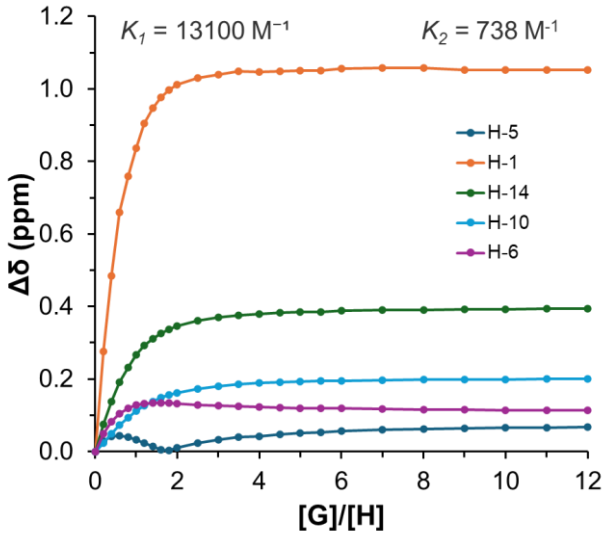


**Figure S65.** Changes in chemical shifts of H-1, H-5, H-6, H-10 and H-14 in the $^{1}$H NMR (400 MHz, DMSO-$d_6$, 298 K) spectra of **3b** (2 mM) after titration with MsONa.

## Tosylate binding studies

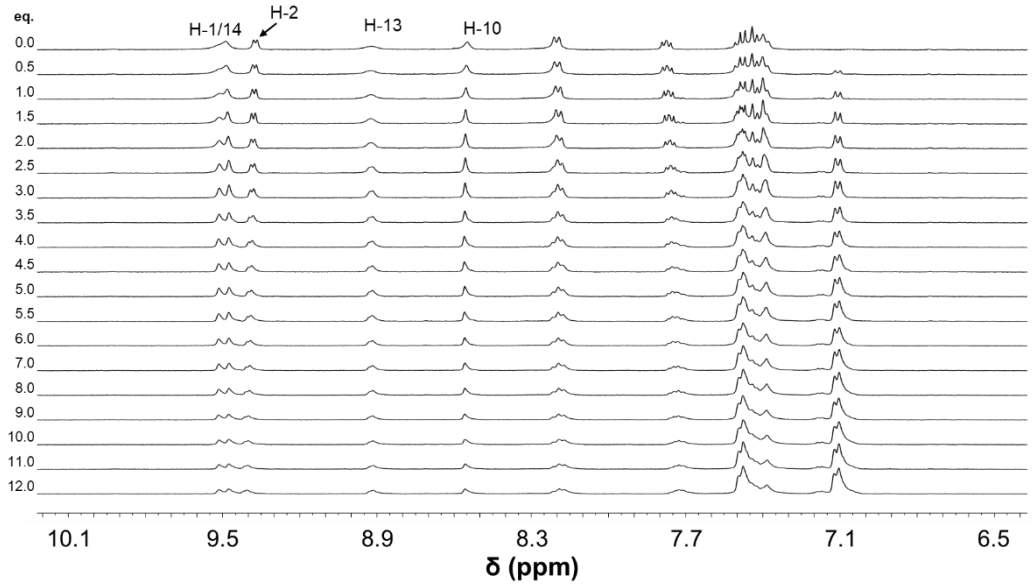


**Figure S66.** $^{1}$H NMR (400 MHz, DMSO-$d_6$, 298 K) spectra for the titration of TsONa into **1a** (2 mM).

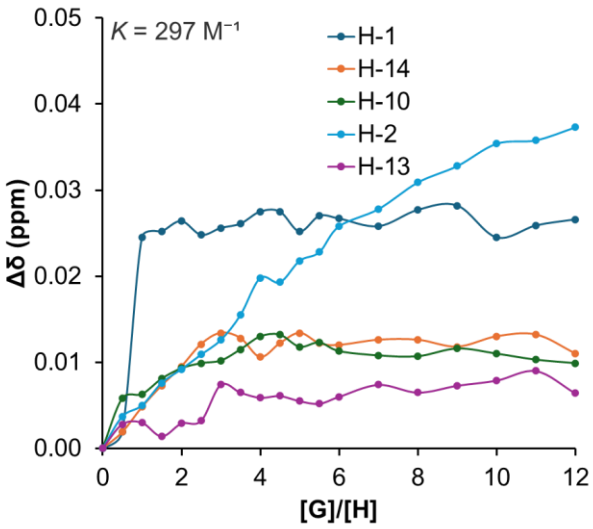


**Figure S67.** Changes in chemical shifts of H-1, H-2, H-10, H-13 and H-14 in the $^{1}$H NMR (400 MHz, DMSO-$d_6$, 298 K) spectra of **1a** (2 mM) after titration with TsONa.

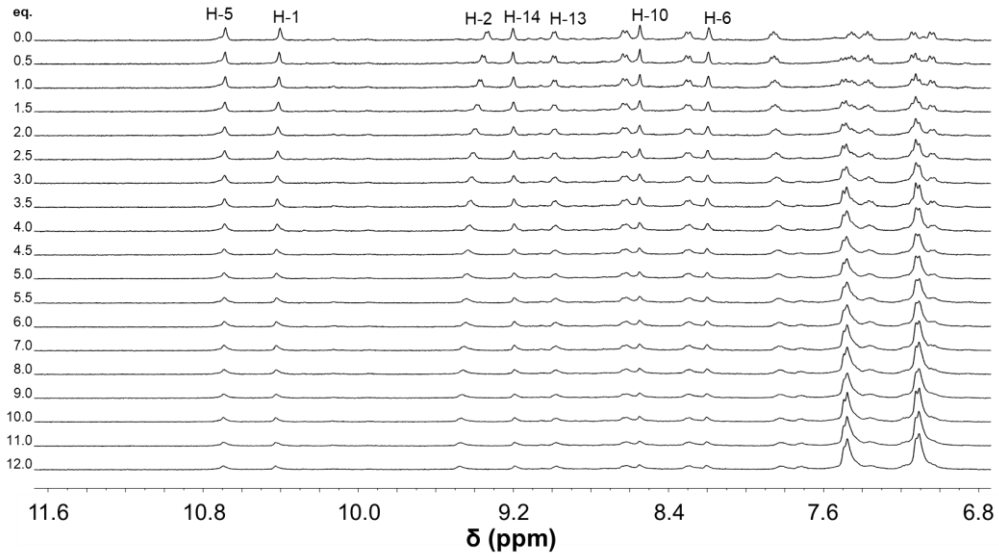


**Figure S68.** $^{1}$H NMR (400 MHz, DMSO-$d_6$, 298 K) spectra for the titration of TsONa into **2a** (2 mM).

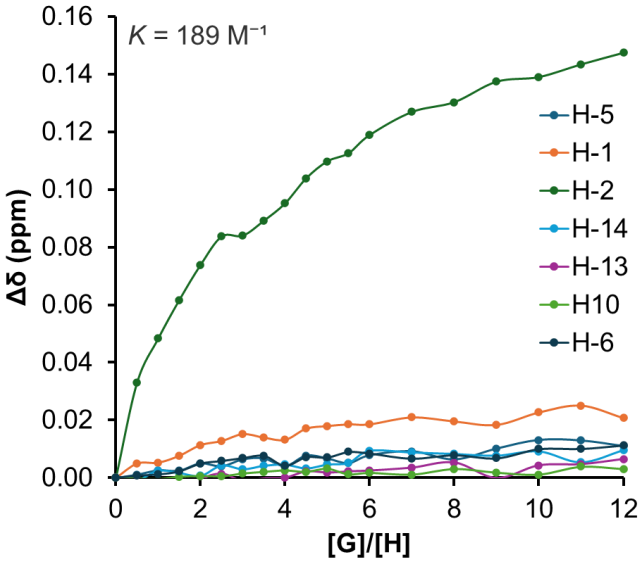


**Figure S69.** Changes in chemical shifts of H-1, H-2, H-5, H-6, H-10, H-13 and H-14 in the $^{1}$H NMR (400 MHz, DMSO-$d_6$, 298 K) spectra of **2a** (2 mM) after titration with TsONa.

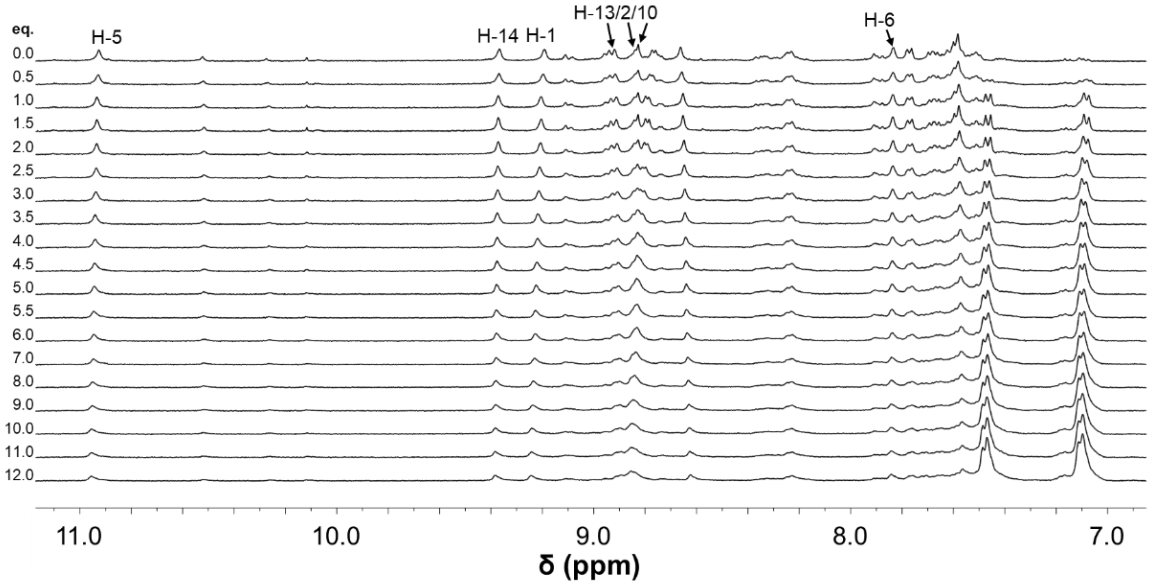


**Figure S70.** $^{1}$H NMR (400 MHz, DMSO-$d_6$, 298 K) spectra for the titration of TsONa into **3a** (2 mM).

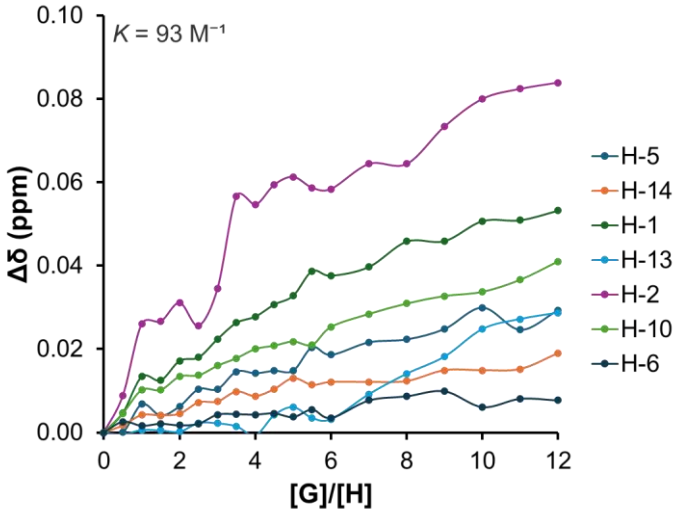


**Figure S71.** Changes in chemical shifts of H-1, H-2, H-5, H-6, H-10, H-13 and H-14 in the $^{1}$H NMR (400 MHz, DMSO-$d_6$, 298 K) spectra of **3a** (2 mM) after titration with TsONa.

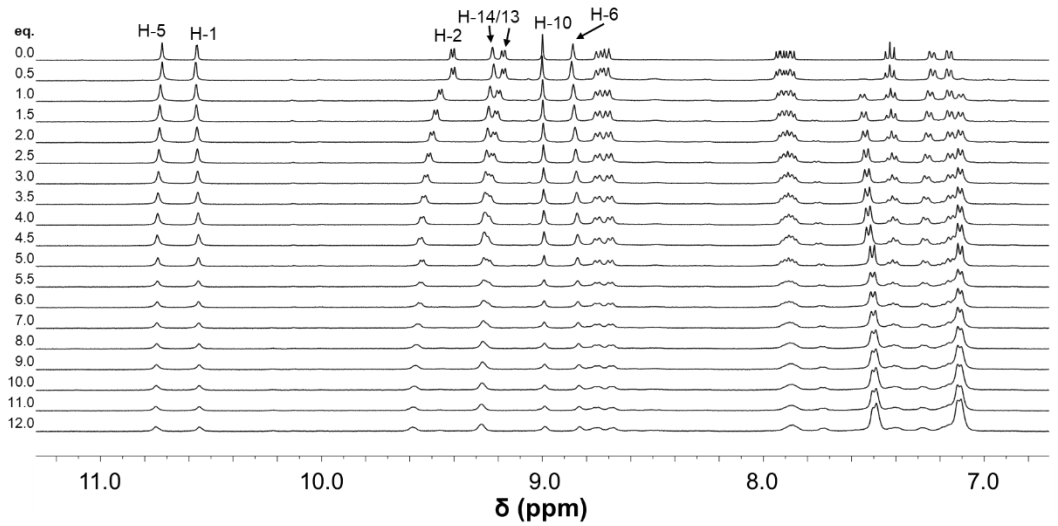


**Figure S72.** $^{1}$H NMR (400 MHz, DMSO-$d_6$, 298 K) spectra for the titration of TsONa into **2b** (2 mM).

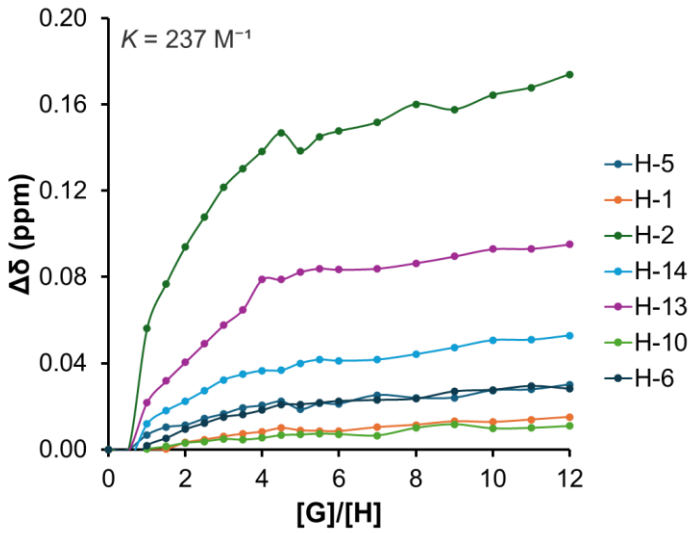


**Figure S73.** Changes in chemical shifts of H-1, H-2, H-5, H-6, H-10, H-13 and H-14 in the $^{1}$H NMR (400 MHz, DMSO-$d_6$, 298 K) spectra of **2b** (2 mM) after titration with TsONa.

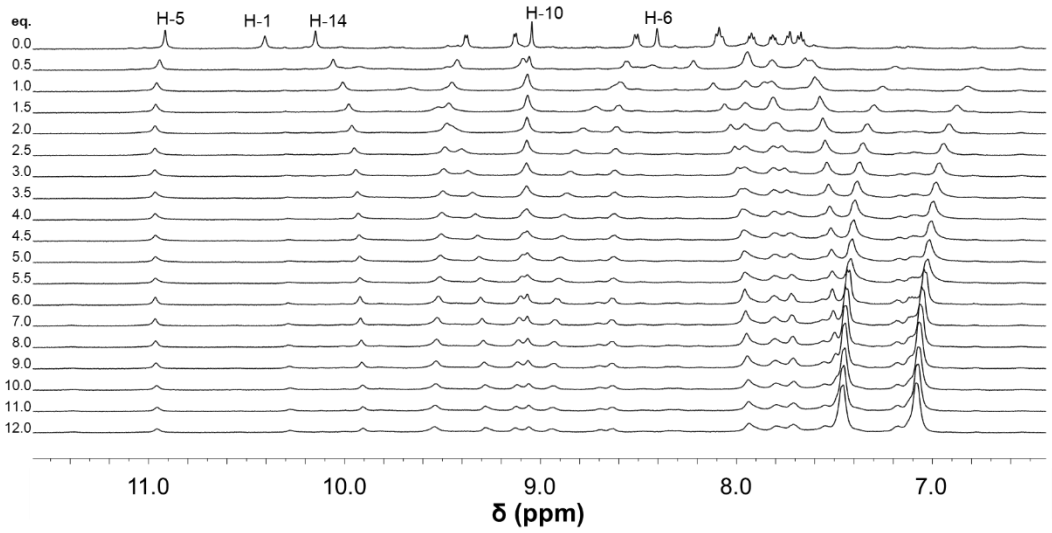


**Figure S74.** $^{1}$H NMR (400 MHz, DMSO-$d_6$, 298 K) spectra for the titration of TsONa into **3b** (2 mM).

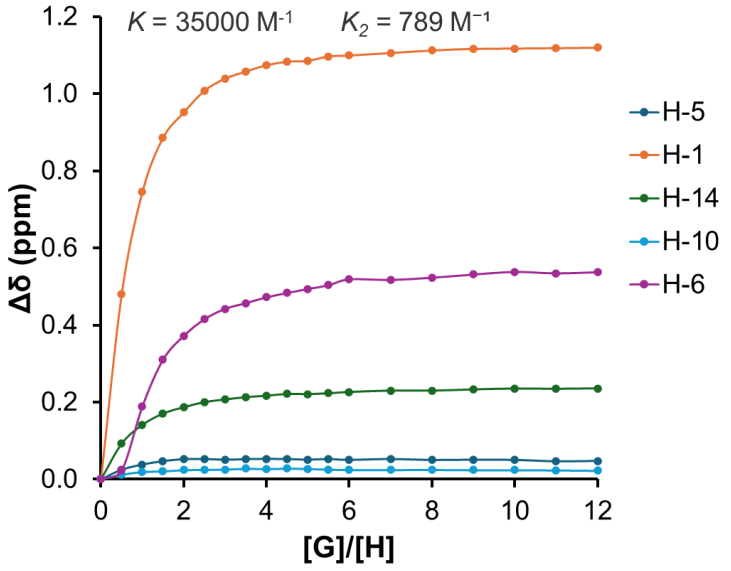


**Figure S75.** Changes in chemical shifts of H-1, H-5, H-6, H-10, and H-14 in the $^{1}$H NMR (400 MHz, DMSO-$d_6$, 298 K) spectra of **3b** (2 mM) after titration with TsONa.

## Cisplatin and 5-fluorouracil as guests

Samples of **1a**–**3a**, **2b** and **3b** were sonicated with ~5 eq. of cisplatin or 5-fluorouracil (5-FU) in MeCN-$d_3$ for 30 min. Then the samples were filtered and $^1$H NMR spectra were recorded immediately. MSAs **1a**–**3a** were unstable in MeCN-$d_3$ and, therefore, adequate spectra could not be obtained for these compounds or with guests.

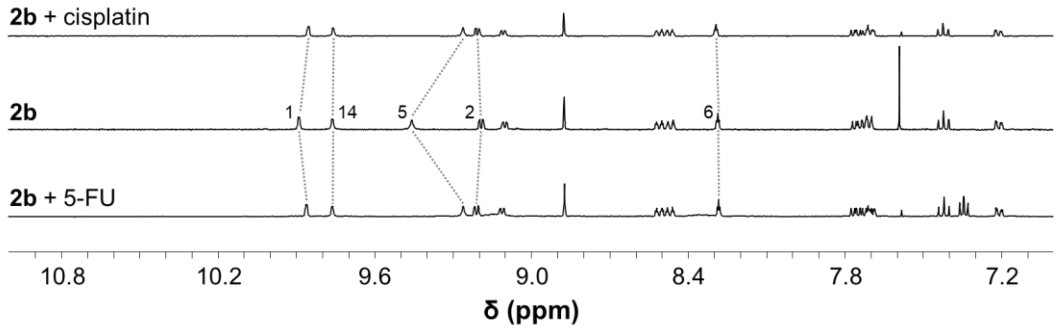


**Figure S76.** $^1$H NMR spectra (400 MHz, MeCN-$d_3$, 298 K) of **2b** and the CISs seen in mixtures with 5-FU and cisplatin.

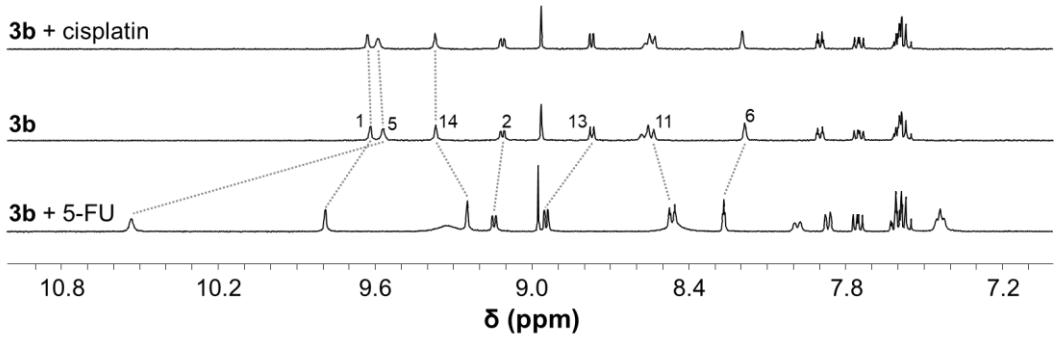


**Figure S77.** $^1$H NMR spectra (400 MHz, MeCN-$d_3$, 298 K) of **3b** and the CISs seen in mixtures with 5-FU and cisplatin.

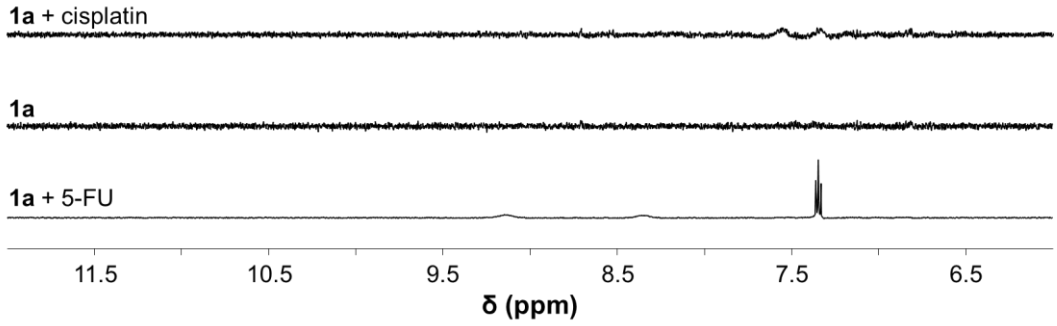


**Figure S78.** $^{1}$H NMR spectra (400 MHz, MeCN-$d_3$, 298 K) of **1a** and mixtures with 5-FU and cisplatin.

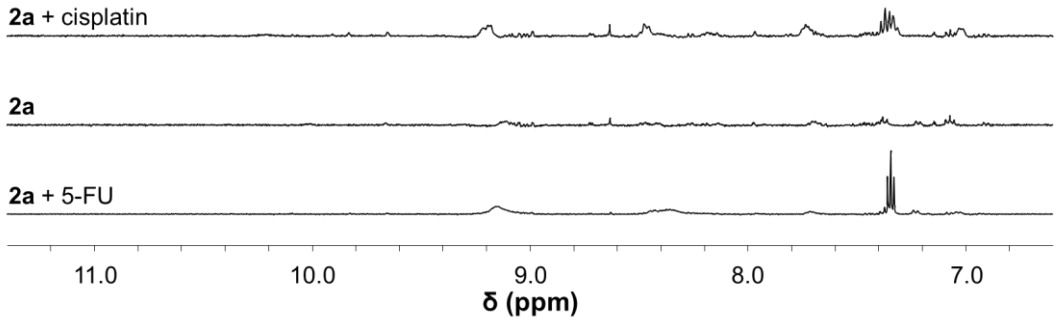


**Figure S78.** $^{1}$H NMR spectra (400 MHz, MeCN-$d_3$, 298 K) of **2a** and mixtures with 5-FU and cisplatin.

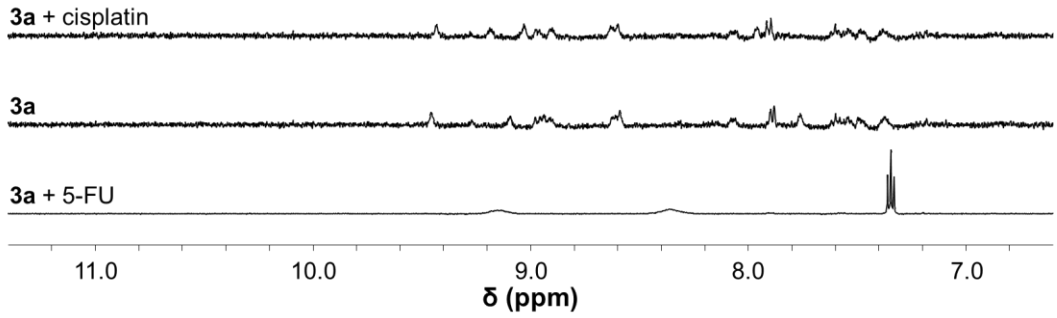


**Figure S79.** $^{1}$H NMR spectra (400 MHz, MeCN-$d_3$, 298 K) of **3a** and mixtures with 5-FU and cisplatin.

**Table S2.** Binding constants found by $^{1}$H NMR spectroscopy for the binding of mesylate or tosylate to **1a**–**3a**, **2b** and **3b**, calculated using supramolecular.org.[14,15]

| | **Mesylate** | | **Tosylate** | |
|---|---|---|---|---|
| | $K_1$ / $M^{-1}$ | $K_2$ / $M^{-1}$ | $K_1$ / $M^{-1}$ | $K_2$ / $M^{-1}$ |
| **1a** | 75 | - | 297 | - |
| **2a** | 209 | - | 189 | - |
| **3a** | 314 | - | 93 | - |
| **2b** | 279 | - | 237 | - |
| **3b** | 13100 | 738 | 35000 | 789 |

**Table S3.** Summary of the guest binding observed for supramolecular architectures **1a**–**3b**.

| **Compound** | **Guest Binding** | | | |
|---|---|---|---|---|
| | Mesylate | Tosylate | 5-FU | cisplatin |
| **1a** | exo | exo | n.d.[a] | n.d.[a] |
| **2a** | exo | exo | n.d.[a] | n.d.[a] |
| **3a** | endo | exo | n.d.[a] | n.d.[a] |
| **1b** [16] | n.d. | n.d. | endo | endo |
| **2b** | endo | endo | exo | exo |
| **3b** | endo | endo | endo | endo |

n.d., not determined; [a] not stable in acetonitrile.

## Molecular structure determination

**Table S4.** Measurement parameters for the molecular structures of **a**, **2a**, **3a**, **2b** and **3b**.

| **Parameter** | **Compound** | | | | |
|---|---|---|---|---|---|
| | **a** | **2a** | **3a** | **2b** | **3b** |
| Method | MicroED | SC-XRD | SC-XRD | SC-XRD | MicroED |
| CCDC number | 2366826 | 2366827 | 2366829 | 2366828 | 2366830 |
| Empirical formula | $C_{24}H_{20}Cl_2N_4O_4Ru$ | $C_{74}H_{62}B_4Cl_2F_{16}N_{16}O_5PdRuS$ | $C_{100}H_{112}B_4Cl_2F_{16}N_{20}O_{16}PdRu$ | $C_{80}H_{80}B_4F_{16}N_{16}O_8PdPtS_4$ | $C_{80}H_{58}B_4F_{16}N_8O_5PdPt$ |
| Formula weight | 600.42 | 1913.06 | 2475.786 | 2170.57 | 1860.11 |
| Temperature/K | 298.15 | 109.99(14) | 100.00(10) | 100.0(2) | 298 |
| Crystal system | orthorhombic | tetragonal | tetragonal | monoclinic | tetragonal |
| Space group | *Pnnn* | *P4/n* | *P4/ncc* | $P2_1/n$ | *P4/n* |
| a/Å | 9.1800(2) | 17.5837(1) | 18.90303(5) | 19.8976(2) | 15.8500(2) |
| b/Å | 10.4500(2) | 17.5837(1) | 18.90303(5) | 18.6335(2) | 15.8500(2) |
| c/Å | 12.4200(2) | 16.0276(2) | 32.38790(13) | 23.8075(2) | 17.7400(2) |
| α/° | 90 | 90 | 90 | 90 | 90 |
| β/° | 90 | 90 | 90 | 95.0374(9) | 90 |
| γ/° | 90 | 90 | 90 | 90 | 90 |
| Volume/Å$^3$ | 1191.46(4) | 4955.52(8) | 11572.99(6) | 8792.79(15) | 4456.69(12) |
| Z | 2 | 2 | 4 | 4 | 2 |
| $\rho_{calc}$g/cm$^3$ | 1.674 | 1.282 | 1.421 | 1.640 | 1.386 |
| μ/mm$^{-1}$ | 0.000 | 4.087 | 3.550 | 6.326 | 0.000 |
| F(000) | 214.0 | 1924.0 | 5095.9 | 4352.0 | 635.0 |
| Crystal size/mm$^3$ | 0.001 × 0.001 × 0.001 | 0.14 × 0.12 × 0.1 | 0.18 × 0.18 × 0.18 | 0.13 × 0.12 × 0.06 | 0.001 × 0.001 × 0.001 |

**Table S4.** Cont.'d

| Radiation | electron (λ = 0.0251 Å) | Cu Kα (λ = 1.54184 Å) | Cu Kα (λ = 1.54184 Å) | Cu Kα (λ = 1.54184 Å) | electron (λ = 0.0251 Å) |
|---|---|---|---|---|---|
| 2Θ range for data collection/° | 0.18 to 1.69 | 7.11 to 135.424 | 8.58 to 135.44 | 7.456 to 135.48 | 0.152 to 1.69 |
| Index ranges | -10 ≤ h ≤ 10, -12 ≤ k ≤ 12, -14 ≤ l ≤ 14 | -20 ≤ h ≤ 21, -19 ≤ k ≤ 18, -18 ≤ l ≤ 19 | -23 ≤ h ≤ 22, -22 ≤ k ≤ 23, -39 ≤ l ≤ 39 | -23 ≤ h ≤ 23, -22 ≤ k ≤ 22, -25 ≤ l ≤ 28 | -18 ≤ h ≤ 18, -18 ≤ k ≤ 18, -19 ≤ l ≤ 19 |
| Reflections collected | 11932 | 23009 | 349032 | 121705 | 36238 |
| Independent reflections | 1011 [Rint = 0.5750, Rsigma = 0.2478] | 4500 [Rint = 0.0344, Rsigma = 0.0233] | 5252 [$R_{int}$ = 0.0330, $R_{sigma}$ = 0.0065] | 15924 [Rint = 0.0469, Rsigma = 0.0261] | 3460 [$R_{int}$ = 0.2752, $R_{sigma}$ = 0.1535] |
| Data/restraints/parameter | 1011/0/82 | 4500/0/236 | 5252/40/341 | 15924/72/1242 | 3460/288/215 |
| Goodness-of-fit on F2 | 1.272 | 1.072 | 1.068 | 1.018 | 1.852 |
| Final R indexes [I>=2σ (I)] | R1 = 0.1895, wR2 = 0.4163 | R1 = 0.0534, wR2 = 0.1522 | R1 = 0.0465, wR2 = 0.1379 | R1 = 0.0372, wR2 = 0.0943 | $R_1$ = 0.2183, $wR_2$ = 0.4980 |
| Final R indexes [all data] | R1 = 0.2986, wR2 = 0.5053 | R1 = 0.0610, wR2 = 0.1602 | R1 = 0.0473, wR2 = 0.1388 | R1 = 0.0442, wR2 = 0.0987 | $R_1$ = 0.2675, $wR_2$ = 0.5185 |
| Largest diff. peak/hole / e $Å^{-3}$ | 0.21/-0.37 | 0.83/-0.67 | 0.73/-0.72 | 1.51/-1.06 | 0.69/-0.29 |

**Table S5.** Selected average bond lengths observed for MSAs **2a**, **3a**, **2b** and **3b** in comparison to *trans*-[Ru(3-PA)$_4$Cl$_2$], *trans*-[Ru(pyridine)$_4$Cl$_2$],[17] and **1b**.[2]

| **Bond** | **Bond length / Å** | | | | | | |
|---|---|---|---|---|---|---|---|
| | *trans*-[Ru(pyridine)$_4$Cl$_2$] [17] | *trans*-[Ru(3-PA)$_4$Cl$_2$] **a** | **2a** | **3a** | **1b** [2] | **2b** | **3b** |
| Ru–Cl | 2.4070(11) | 2.413(11) | 2.405(2) | 2.4044(13) | – | – | – |
| Ru–N | 2.075(2) | 2.093(12) | 2.083(4) | 2.072(2) | – | – | – |
| Pd–N | – | – | 2.040(3) | 2.031(2) | 2.02(3) | 2.018(3)* | 2.093(10) |
| Pt–N | – | – | – | – | 2.06(3) | 2.012(3) ‡ | 2.057(12) |
| Ru/Pt···Pd | – | – | 10.4218(7) | 10.3565(5) | 11.52(2) | 11.5132(6) | 9.496(12) |

* Four distances from 2.018(3) to 2.036(3) Å; ‡ Four distances from 2.012(3) to 2.022(3) Å.

**Colour codes** used to indicate the atoms in all the molecular structures: C: grey, N: blue, O: red, Cl: green, Ru: light orange, Pd: dark red, Pt: amber, S: pale yellow.

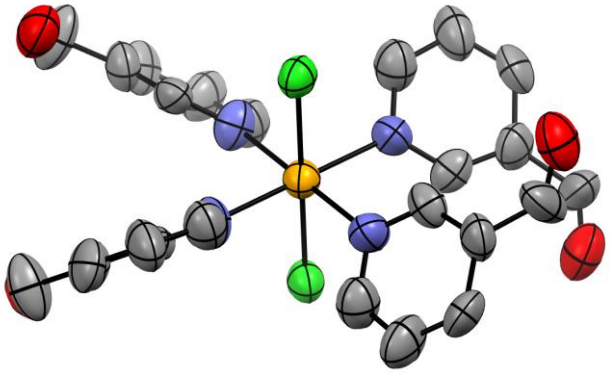

**Figure S80.** Molecular structure of *trans*-[Ru(3-PA)$_4$Cl$_2$] **a** as determined by micro-ED drawn at 50% probability level.

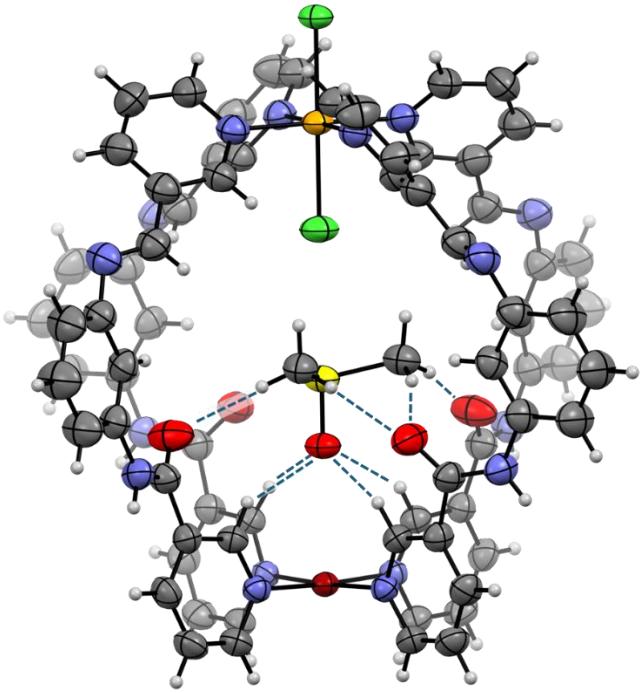

**Figure S81.** Molecular structure of one of the enantiomers of **2a** drawn at 50% probability level. The structure features disordered DMSO molecules in the centre of the cavity one of which is shown and the H bonds are indicated with dashed lines. Counteranions were removed for clarity.

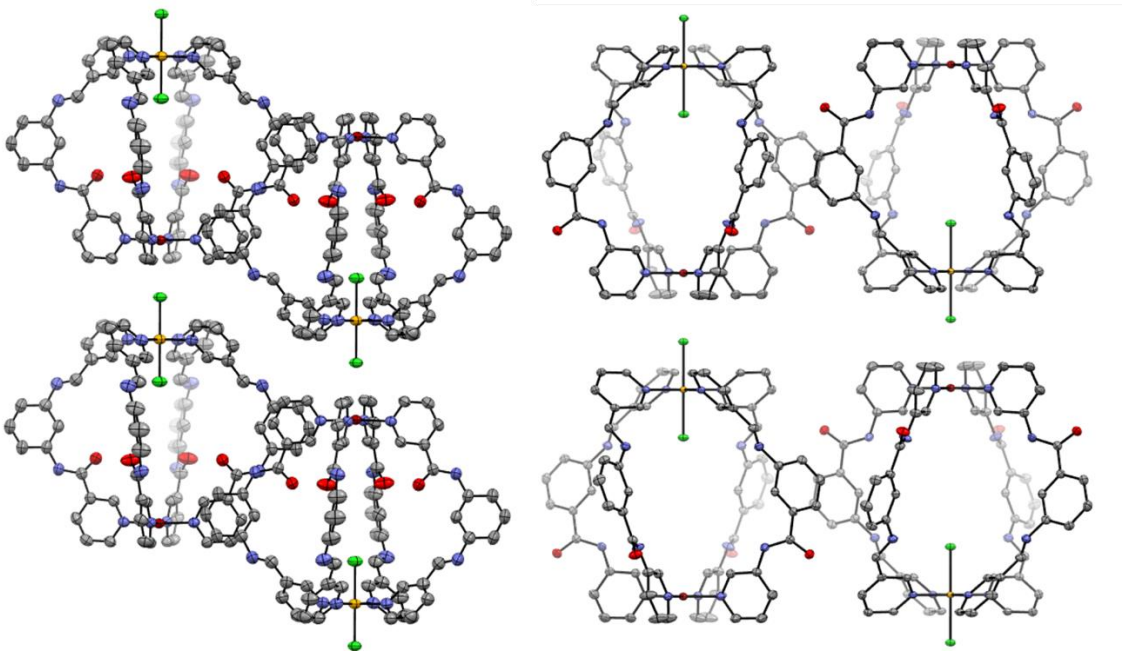

**Figure S82.** Enantiomers of helicate structures of **2a** (left) and **3a** (right) arranged in antiparallel strings with the Ru–Cl bonds pointing towards the Pd centres of the adjacent molecule of **2a** or **3a**.

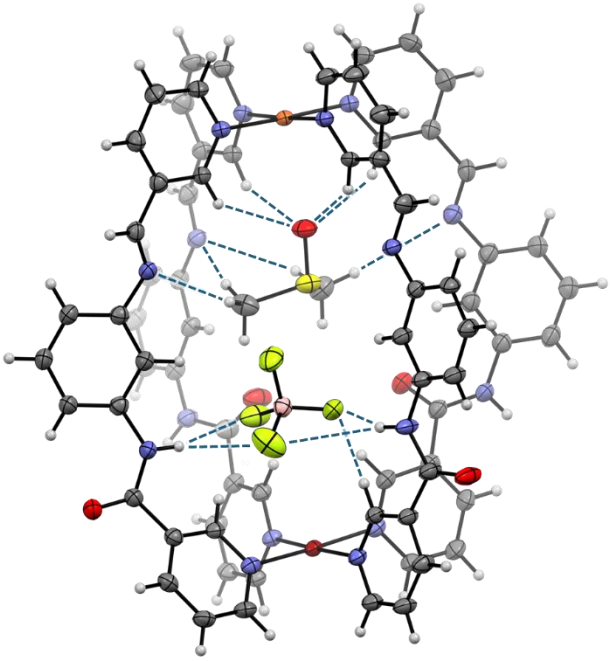

**Figure S83.** Molecular structure of a molecule of **2b** drawn at 50% probability level. The structure features co-crystallised DMSO and $BF_4^-$ in the centre of the cavity and the H bonds are indicated with dashed lines. Other co-crystallised solvent molecules and counteranions were removed for clarity.

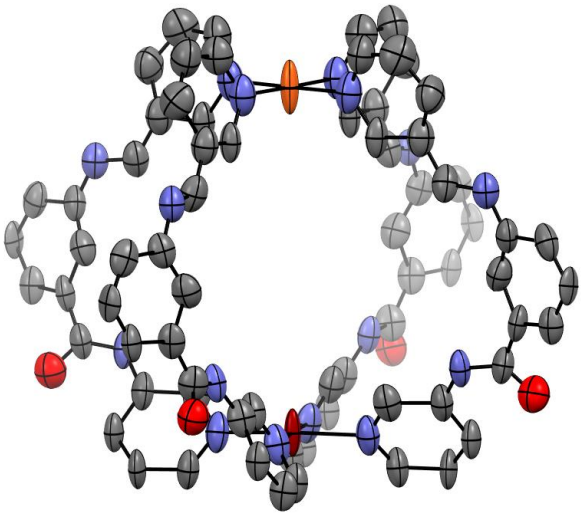

**Figure S84.** Molecular structure of a molecule of **3b** drawn at 50% probability level. Hydrogen atoms, co-crystallised solvent molecules and counteranions were removed for clarity.

## Host-guest MMFF models

All Merck Molecular Force Field (MMFF) models were generated in SPARTAN '24®.[18] Cages **1a**–**3a** were modelled with mesylate and tosylate bound, while **2b** and **3b** were modelled with mesylate, tosylate, 5-fluorouracil and cisplatin due to the CISs seen in the $^{1}$H NMR spectra of mixtures containing these guests. Guest binding was modelled to reflect the interactions observed by NMR spectroscopy. In the case of **3b**, 2 equivalents of mesylate and tosylate were modelled to reflect the guest-binding titration data. All structures were energy minimised to give optimised host-guest models. Carbon atoms of guest molecules are coloured black to differentiate from those of the host (grey).

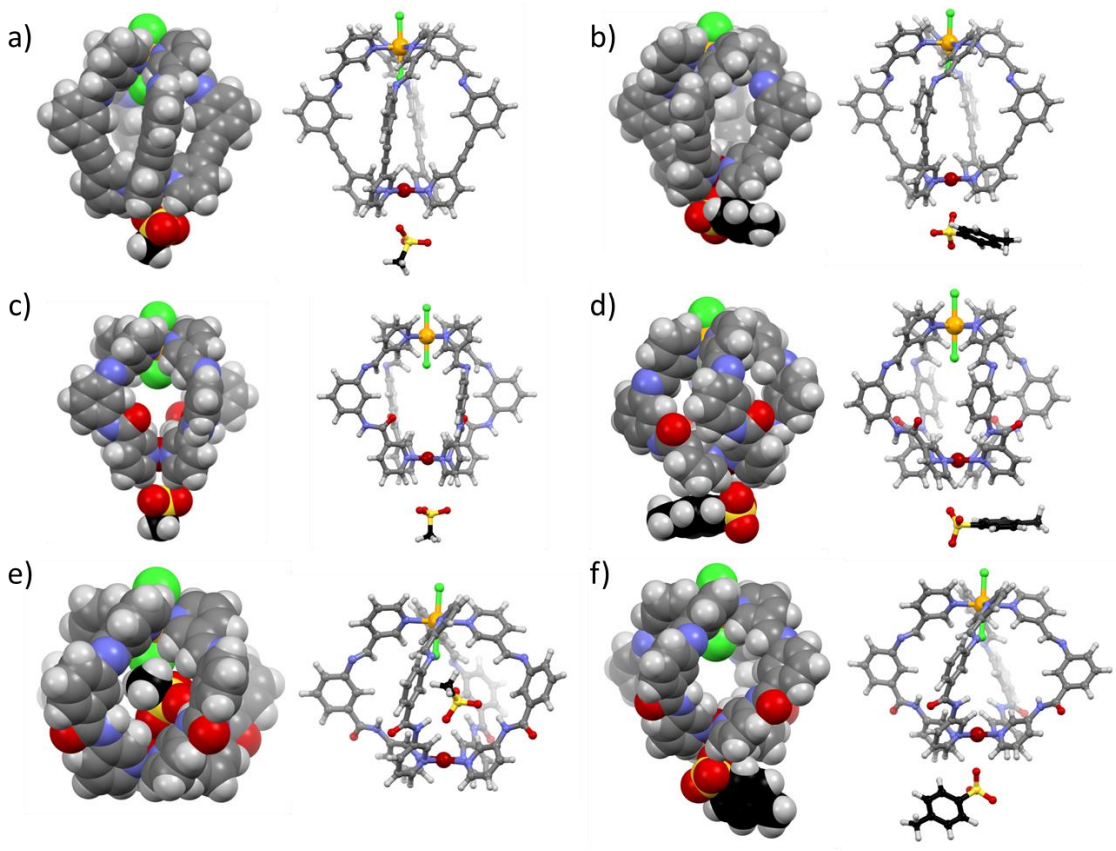


**Figure S85.** MMFF Spartan '24® models of a) MsO⊂**1a**, b) TsO⊂**1a**, c) MsO⊂**2a**, d) TsO⊂**2a**, e) MsO⊂**3a**, and f) TsO⊂**3a**.

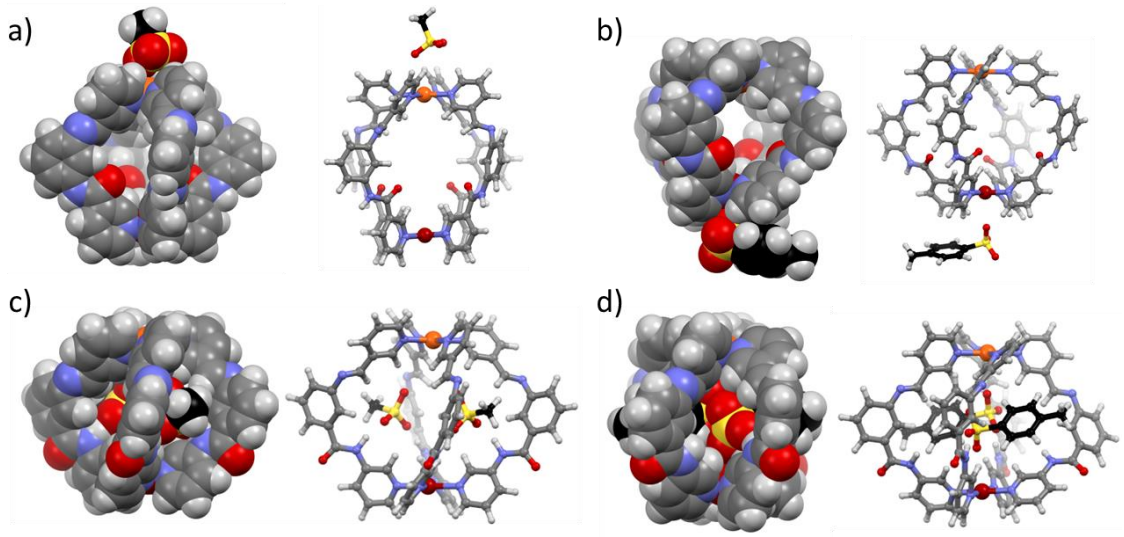


**Figure S86.** MMFF Spartan '24® models of a) MsO⊂**2a**, b) TsO⊂**2a**, c) 2MsO⊂**3b**, and d) 2TsO⊂**3b.**

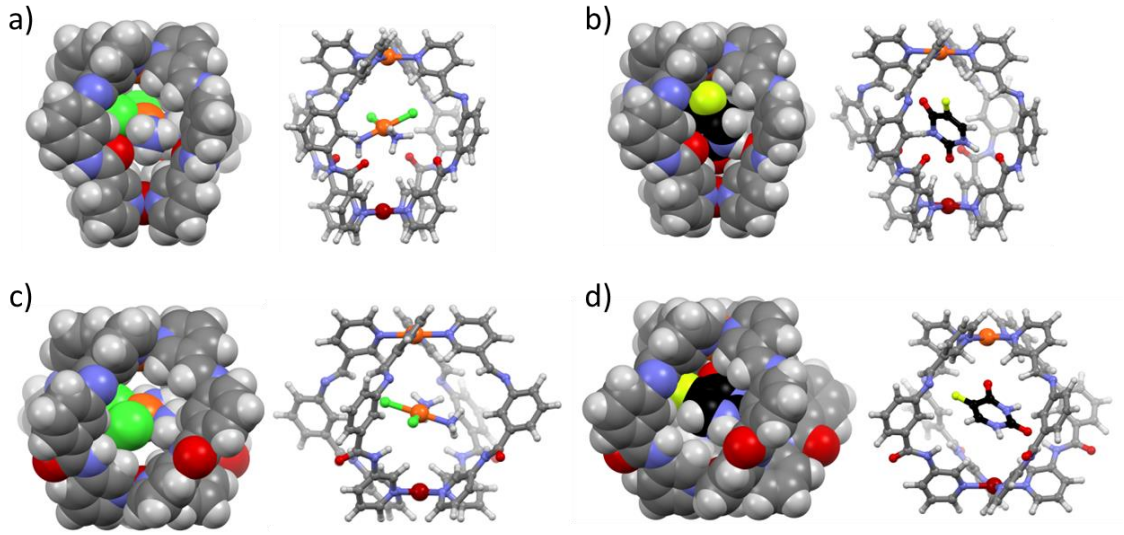


**Figure S87.** MMFF Spartan '24® models of a) cisplatin⊂**2a**, b) 5-fluorouracil⊂**2a**, c) cisplatin⊂**3b**, and d) 5-fluorouracil⊂**3b.**

## Reactions with $AgBF_4$

To test the lability towards silver salts of the chlorides bound to ruthenium for **1a**–**3a**, solutions in DMSO-$d_6$ (2 mM) were prepared and 500 µL was transferred to an NMR tube. 20 µL of a $AgBF_4$ solution in DMSO-$d_6$ (100 mM, 2 eq) was then added and the samples were analysed at time intervals of 1, 24, 72 h, and 7 d.

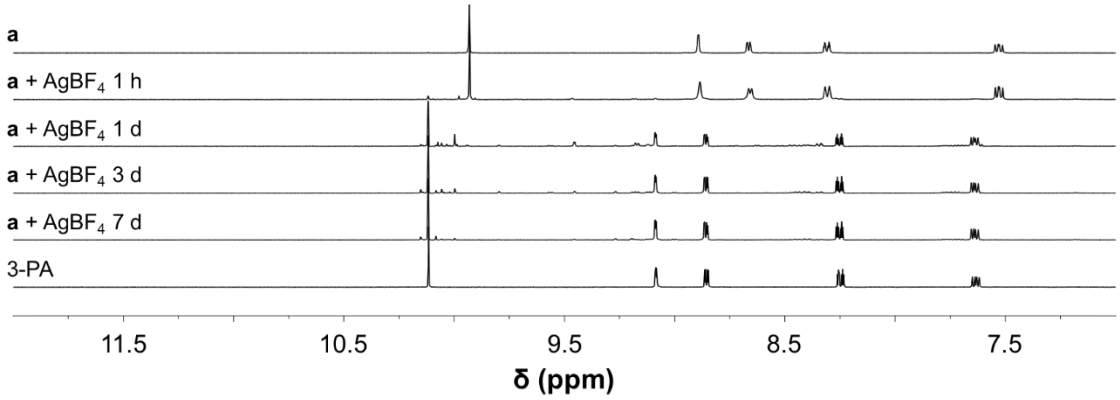


**Figure S88.** $^1$H NMR spectra (400 MHz, DMSO-$d_6$, 298 K) of $[Ru(3\text{-}PA)_4Cl_2]$ **a** and after addition of $AgBF_4$ at 1, 24, 72 h, and 7 days, with comparison to the ligand (3-PA).

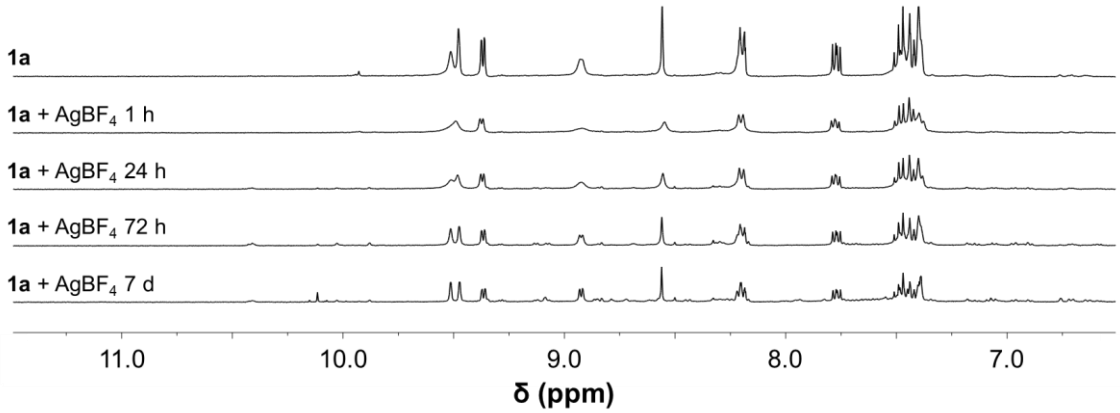


**Figure S89.** $^1$H NMR spectra (400 MHz, DMSO-$d_6$, 298 K) of **1a** and after addition of $AgBF_4$ at 1, 24, 72 h, and 7 days.

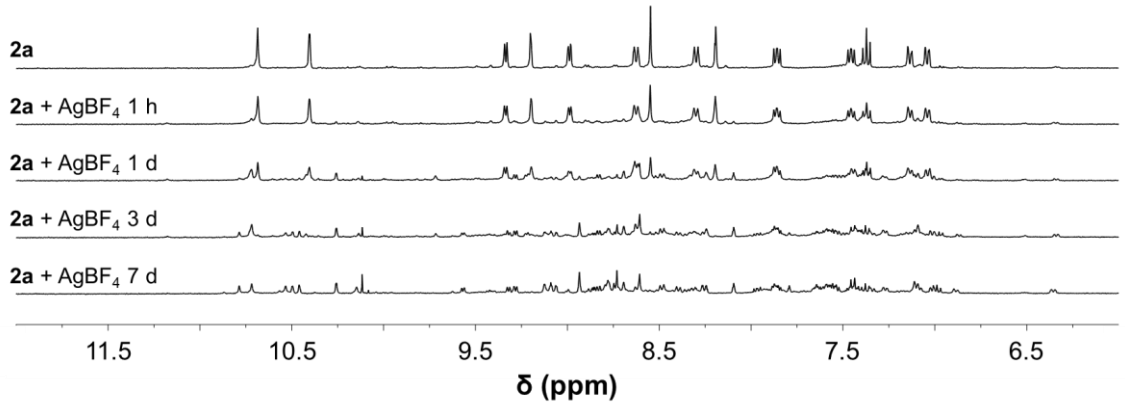


**Figure S90.** $^{1}$H NMR spectra (400 MHz, DMSO-$d_6$, 298 K) of **2a** and after addition of AgBF4 at 1, 24, 72 h, and 7 days.

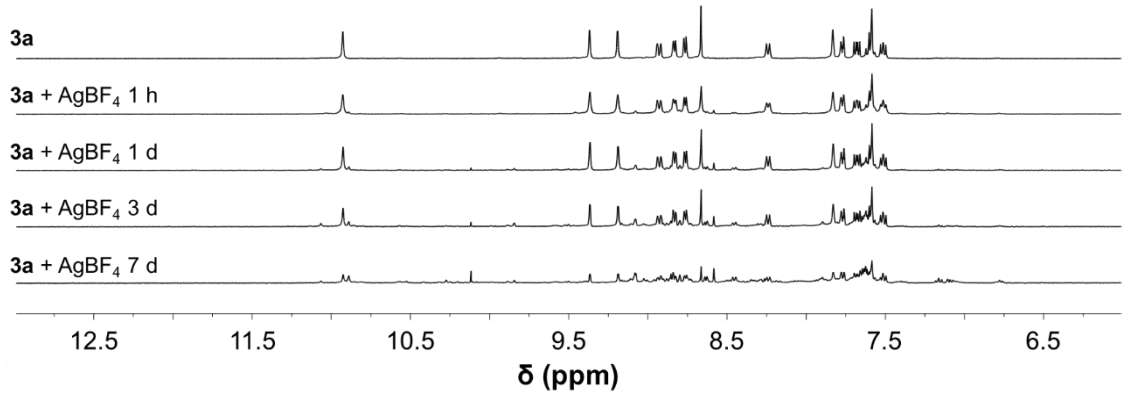


**Figure S91.** $^{1}$H NMR spectra (400 MHz, DMSO-$d_6$, 298 K) of **3a** and after addition of $AgBF_4$ at 1, 24, 72 h, and 7 days.

## References


1 J. E. M. Lewis, E. L. Gavey, S. A. Cameron and J. D. Crowley, *Chem. Sci.*, 2012, **3**, 778.

2 L. S. Lisboa, J. A. Findlay, L. J. Wright, C. G. Hartinger and J. D. Crowley, *Angew. Chem., Int. Ed.*, 2020, **59**, 11101.

3 F. Mu, S. L. Coffing, D. J. Riese, R. L. Geahlen, P. Verdier-Pinard, E. Hamel, J. Johnson and M. Cushman, *J. Med. Chem.*, 2001, **44**, 441.

4 J. S. Jaswal, S. J. Rettig and B. R. James, *Can. J. Chem.*, 1990, **68**, 1808.

5 G. Sheldrick, *Acta Crystallogr., Sect. A: Found. Adv.*, 2015, **71**, 3.

6 L. J. Bourhis, O. V. Dolomanov, R. J. Gildea, J. A. K. Howard and H. Puschmann, *Acta Crystallogr., Sect. A: Found. Crystallogr.*, 2015, **71**, 59.

7 O. V. Dolomanov, L. J. Bourhis, R. J. Gildea, J. A. K. Howard and H. Puschmann, *J. Appl. Crystallogr.*, 2009, **42**, 339.

8 C. F. Macrae, I. Sovago, S. J. Cottrell, P. T. A. Galek, P. McCabe, E. Pidcock, M. Platings, G. P. Shields, J. S. Stevens, M. Towler and P. A. Wood, *J. Appl. Crystallogr.*, 2020, **53**, 226.

9 *guiEM2EM*, Image Science Software GmbH.

10 Scripps, *Adxv – A Program to Display X-ray Diffraction Images*, (2013).

11 W. Kabsch, *Acta Crystallographica Section D: Biological Crystallography*, 2010, **66**, 125.

12 G. Sheldrick, *Acta Crystallogr., Sect. C: Struct. Chem.*, 2015, **71**, 3.

13 *http://supramolecular.org*

14 P. Thordarson, *Chem. Soc. Rev.*, 2011, **40**, 1305.

15 D. Brynn Hibbert and P. Thordarson, *Chem. Commun.*, 2016, **52**, 12792.

16 L. Lisboa, University of Otago, 2022.

17 M. Trivedi, Y. K. Sharma, R. Nagarajan and N. P. Rath, *J. Mol. Struct.*, 2010, **975**, 335.

18 *Spartan '24*, Wavefunction, Inc.